# MOLECULARLY- IMPRINTED POLYANILINE NANOPARTICLES FOR DETECTION OF ALDRIN

**BY**

**ABIGAIL MBOZI**

**A DISSERTATION SUBMITTED TO THE UNIVERSITY OF ZAMBIA IN PARTIAL FULFILMENT OF THE REQUIREMENTS FOR THE DEGREE OF**

**MASTER OF SCIENCE IN CHEMISTRY**

**THE UNIVERSITY OF ZAMBIA**

**LUSAKA**

**2016**

# DECLARATION

I hereby declare that this dissertation represents my own work, and that to the best of my knowledge, it has not been previously submitted for the award of a degree at this or any other university.

Full Name: Abigail Mbozi.

Signature : .....

Date : .....

# APPROVAL

This dissertation of **Abigail Mbozi** is approved as partial fulfilment of the requirements for the award of the degree of Master of Science in Chemistry by the University of Zambia.

| **Examiner's name** | **Signature** | **Date** |
|---|---|---|
| ..... | ..... | ..... |
| **Examiner I** | | |
| ..... | ..... | ..... |
| **Examiner II** | | |
| ..... | ..... | ..... |
| **Examiner III** | | |
| ..... | ..... | ..... |
| **Supervisor** | | |

# ABSTRACT

Molecularly imprinted polymers are a class of new functional materials that bring about selectivity to chemical sensors that is similar to that found in biological systems. The technique enables the creation of artificial recognition cavities within synthetic polymers that can be used in chemical sensors to detect specific analytes. Molecularly imprinted nanostructured materials of defined shape and size show remarkable properties that can be utilized in different fields of analytical chemistry. The work presented in this dissertation is on the preparation, characterization and evaluation of molecularly imprinted polyaniline nanoparticles that can be used to selectively detect aldrin. Molecularly imprinted polyaniline (MI-PANI) nanoparticles were prepared by inverted emulsion polymerization using aldrin as template and aniline as a functional monomer. Materials prepared were characterized using FTIR, UV/VIS and NMR for structural elucidation. AFM and SEM were used for morphological characterization which revealed that the particles prepared were spherical in nature. SEM further showed that the particles had diameters ranging from 500 nm – 1.5 μm for MI-PANI compared to a size range of 60 nm – 100 nm for non-imprinted particles. Electrical properties were evaluated using a four-point probe coupled to a source meter. Non-imprinted materials showed an electrical conductivity of 4.149 S/cm that reduced to 0.546 S/cm in MI-PANI. The binding capacity of the imprinted nanoparticles was evaluated via re-binding adsorption experiments and the data fitted into the Langmuir adsorption mathematical model. $K_D$ and $B_{max}$ were calculated to be 0.6 ng/μL and 0.799 ng/μL respectively. The selectivity of imprinted nanoparticles was investigated by examining the adsorption characteristics of aldrin and DDT. The distribution co-efficient for DDT and aldrin were found to be 0.76 ng/ng and 1.31 μL/ng respectively indicating that MI-PANI exhibited much stronger binding affinity for aldrin than DDT.

*To the memory of my parents,*

*Mr Alfred Jeff Mbozi and Mrs Caristus Mutafu Mbozi.*

# ACKNOWLEDGEMENTS

My sincere thanks first and foremost go to almighty God for life and good health, without whose presence in my life I can do nothing. I would like to express my appreciation and thanks to my supervisor Dr. Onesmus Munyati for the faith and support that he has shown in me, my co-supervisor Professor Mwindaace Siamwiza for his encouragement and "paternal" leadership in my life. I also would like to express my appreciation and thanks to Dr. Mmantsae Diale (University of Pretoria) for hosting me during my research visit which enabled me carry out most of the characterisation works and also her useful advice and encouragement to complete this project. My sincere thanks also go to Dr. James Nyirenda for his help throughout my chemistry studies. Furthermore, I would like to offer my gratitude to Dr. Shiv Prakash for his leadership as co-ordinator of the postgraduate committee in the Department of Chemistry. My appreciation also goes to Mr Chipo Syabbamba for enabling use of various equipment in the chemistry department. I acknowledge with thanks and appreciation the International Science Programme (ISP) through the Sustainable Chemistry and Environment Programme (SCEP) at the University of Zambia for financial support. Many thanks to Mr Fred-Joe Nambala and Mr Peter Cheuka for their enthusiasm and insightful input in this work. I also would like to thank my MSc colleagues Daka Jimmy, Hanzooma Hatwiko, Shumba Kenny, Pierre Lokadi Luhata, Mwale Simon, Banda Patrick for their help, support, friendship, and for the many interesting and useful discussions. A special thanks to my husband Mr Isaac Dumbe, for having always been so supportive, reassuring and optimistic even when I was not so sure about my progress, my daughter Felicity Dumbe and son Joshua Elijah Dumbe for understanding my absence when I had to work long hours in the lab. And last but not the least, many thanks to my beloved siblings Patience, Angela and Martin for being so supportive during these years.

# TABLE OF CONTENTS

# LIST OF TABLES

# LIST OF FIGURES

# LIST OF ABBREVIATIONS

## Symbols

| | |
|---|---|
| M | Molar (mol/Litre) |
| m | Metre, length |
| m | Milli ($10^{-3}$) |
| λ | Wavelength (nm) |
| g | Gram, mass |
| eV | Electron volt, energy |
| Mol | Mole, amount |
| n | Nano ($10^{-9}$) |
| L | Litre, volume |
| $K_A$ | Association constant (L/mol) |
| $K_D$ | Dissociation constant (mol/L) |
| μ | Micro ($10^{-6}$) |
| C | Centi ($10^{-2}$) |
| S | Siemens |
| % | Percent, Percentage |
| w/w | Weight by Weight |
| H | Hour |
| °C | Degrees Celsius |
| I | Current |
| V | Voltage |
| δ | Chemical shift |
| υ | Frequency |
| θ | Theta (degree angle) |
| α | Selectivity factor |

## Abbreviations

| | |
|---|---|
| AFM | Atomic Force Microscopy |
| AMBN | 2,2' – azobis-(2-isobutyronitrile) |
| AAm | Acrylamide |
| APS | Ammonium persulphate |
| BFA | L,D-Boc-Phenylalanine anilid |
| COOH | Carboxylic acid |
| CP(s) | Conducting Polymer(s) |
| DMF | Dimethylformamide |
| DVB | Divinylbenzene |
| Eg | Band gap |
| EGDMA | Ethylene glycol dimethacrylate |
| Eb | Emeraldine base |
| Es | Emeraldine salt |
| Fg | Fermi Level |
| FTIR | Fourier Transform Infra Red |
| GC–MS | Gas chromatography Mass Spectrometry |
| GC-TOF MS | Gas chromatography time of fight Mass Spectrometry |
| HCl | Hydrochloric Acid |
| HOMO | Highest Occupied Molecular Orbital |
| $^{1}$H-NMR | Proton Nuclear Magnetic Resonance |
| HPLC | High Performance Liquid Chromatography |
| HPLC-UV | High performance Liquid Chromatography Ultraviolet |
| I-V | Current –Voltage |
| KBr | Potassium Bromide |
| LE | Leucoemeraldine |
| LIN | Linuron |
| LUMO | Lowest Unoccupied Molecular Orbital |
| MAA | Methacrylic Acid |
| MIP | Molecularly Imprinted Polymer |
| MIP NP(s) | Molecularly Imprinted Polymer Nanoparticle (s) |

| | |
|---|---|
| MIP - SPE | Molecularly Imprinted Solid Phase Extraction |
| MI-PANI | Molecularly Imprinted Polyaniline |
| MIT | Molecular Imprinting Technique |
| NIP(s) | Non imprinted polymer(s) |
| NP(s) | Nanoparticle(s) |
| OCP(s) | Organochlorine Pesticides(s) |
| OPP(s) | Organophosphorus Pesticide(s) |
| O/W | Oil-Water |
| PANI | Polyaniline |
| POP(s) | Persistent Organic Pollutant(s) |
| ppm | Parts per million |
| SEM | Scanning Electron Microscopy |
| SDS | Sodium dodecyl sulphate |
| TEM | Transmission Electron Microscopy |
| TMED | *N*,*N*,*N'*,*N'*- tetramethylenethylenediamine |
| TFMAA | Trifluormethacrylic acid |
| TPA | Triphenylamine |
| UV-VIS | Ultra Violet Visible |
| XRD | X -ray Diffraction |

# CHAPTER 1

# INTRODUCTION

## 1.1 Background

The reported accumulation of persistent organic pollutants (POPs) [1] , in particular organochlorine pesticides (OCPs) in the environment resulting from their use in the agriculture and public health sectors has continued to raise concern. This has driven the development of low cost, easy to use devices that make use of novel smart materials with high specificity, selectivity and sensitivities for analytes in the sensing technologies. More specifically, innovative methods for the synthesis of advanced *"tailor-made"* functional materials with specific recognition capacity and long-term performance stability are demanded. One of the most promising classes of new and highly selective functional materials are molecularly imprinted polymers (MIPs) [2]. MIPs are one of the leading contenders in chemical sensor applications, combining selective recognition with chemical strength.

Although the use of conducting polymers (CPs) as transducers in chemical sensors has been widely described in literature [3], their associated sensing devices have been limited due to lack of selectivity to target analytes. With the evolution of molecular imprinting techniques (MIT), CPs can be chemically functionalized such that highly specific recognition sites are built within the polymer matrix resulting in increase in selectivity. Integration of molecularly imprinted conducting polymers as sensitive layers in chemical sensors provides a viable route for development of devices for selective and sensitive detection of environmental pollutants. Figure 1 shows examples of structures of persistent organic pollutants commonly used in agriculture and health sectors.

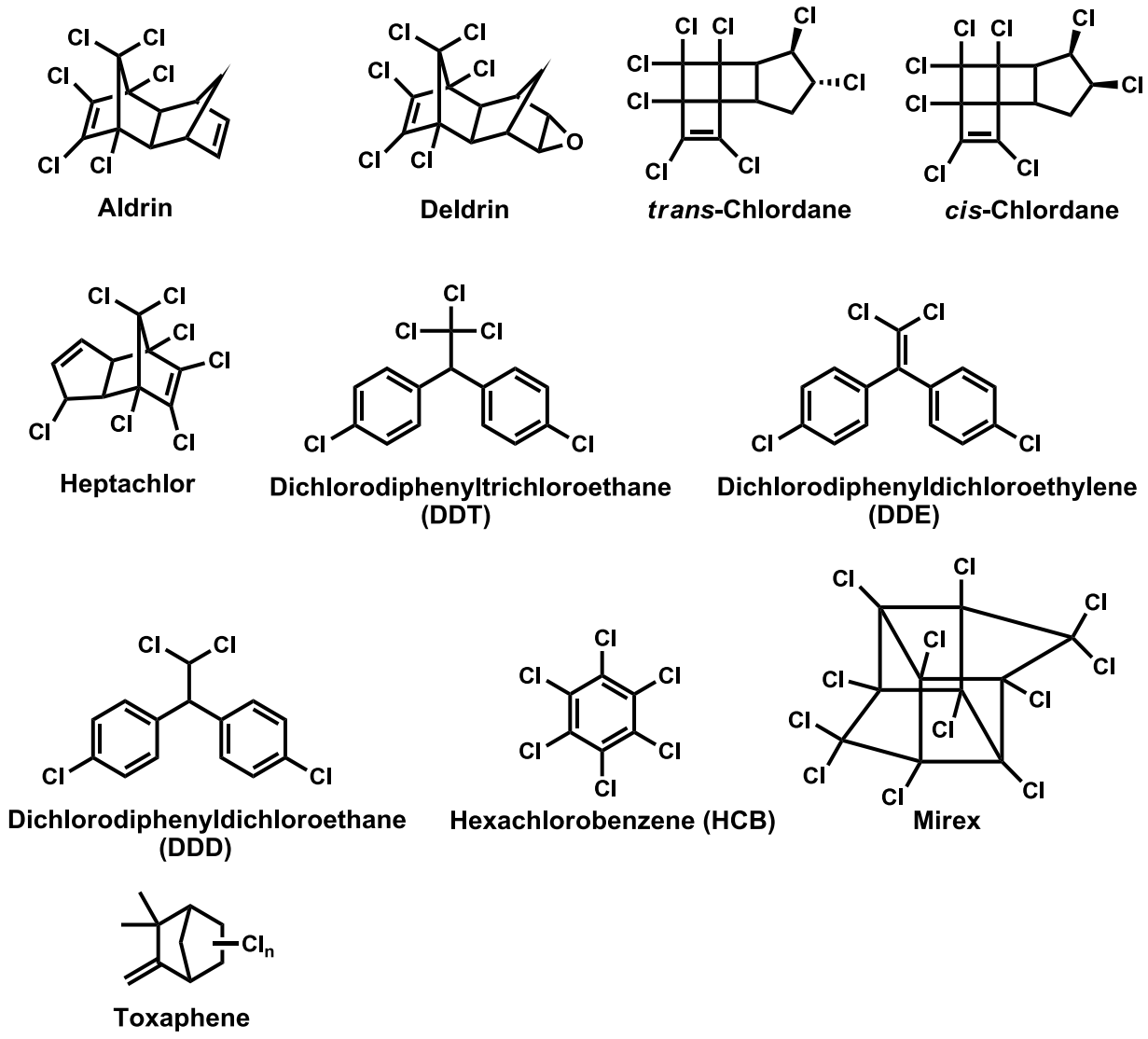


**Figure 1: Structures of common persistent organic pollutants (POPs).**

Molecularly imprinted polymers (MIPs) are usually synthesized by bulk polymerisation of monomers in the presence of templates, subsequently crushing or grinding, sieving and sedimenting the polymer obtained. However, this process is tedious, time consuming and the particles obtained show irregular shapes and size limiting their applicability. In addition, the interaction sites created in the MIPs are destroyed during grinding thereby reducing their loading and recognition. Polymerisation strategies such as emulsion and precipitation polymerisation [2] are well-suited methods to obtain particles of defined shape and with desired characteristics. Particularly, emulsion polymerization has gained attention due to better control of particle sizes and morphologies. MIP particles can be easily

obtained using emulsion polymerisation, the size can be easily controlled and their integrity maintained. In addition, the nano-MIPs obtained offer properties such as increased sensitivity due to high surface area of the particles.

## 1.2 Statement of Problem

Monitoring and analysis of trace levels of persistent organic pollutants in particular organochlorine pesticides are essential for environmental control and protection of human health. Several analytical methods, such as spectrophotometry, liquid chromatography or solid phase micro extraction coupled to gas chromatography mass spectrometry (GC–MS), have been used for the determination of these pesticides. However, these generally require a high degree of expertise. In addition, these methods are associated with high cost equipment and running costs. Chemical sensors have potential to offer lower cost detection systems requiring lower levels of expertise and much shorter response times. The challenges that face chemical sensors include poor selectivity and reversibility. The development of a molecularly imprinted polymer (MIP) based chemical sensor constitutes an alternative for the rapid, sensitive and selective determination of the target analytes.

## 1.3 Significance of Study

Polymer based chemical sensors have potential to offer lower cost, low power portable sensing devices with rapid feedbacks and responses. Environmental monitoring in many developing countries is limited (in part) by the lack of affordable equipment. This creates data gaps, nationally and in the global scenario, as to the levels of pollutants that may be present in the environment. It is anticipated that such devices will enable regular and effective monitoring of such organic pollutants that have adverse impact on environmental and human health.

## 1.4 Objectives

The overall objective of this study was to synthesise, characterise and evaluate molecularly imprinted polyaniline (MI- PANI) nanoparticles (NPs) for the selective adsorption and detection of aldrin.

## 1.5 Specific objectives

The specific objectives of the study were:

a) To optimise the conditions for synthesis of conducting molecularly imprinted polyaniline (MI-PANI) and non- imprinted polyaniline.
b) To characterize the material synthesized in terms of size and shape.
c) To evaluate the electrical, optical and morphological properties of the synthesized MI- PANI and neat polyaniline.
d) To evaluate the sensing characteristics of the MI- PANI in terms of sensitivity and selectivity.

## 1.6 Dissertation outline

Chapter 2 gives the theoretical background of conducting polymers as well as the conduction mechanism. It also extends to discuss conducting polymer nanostructures with an emphasis on polyaniline which is the polymer under study. Chapter 3 gives a review of literature on molecular imprinting techniques and also gives a description of preparation of molecularly imprinted nanoparticles. The discussion is not intended to be a complete review but rather to highlight current efforts by several "researchers" in nano-MIP fabrication and their application in pesticide analysis. The experimental techniques used during the course of this work are explained in chapter 4 while chapter 5 contains discussion of the results that include FTIR, XRD and UV-VIS for structure analysis. Surface morphology analysis from SEM and AFM results and conductivity measurements are also discussed. Furthermore, results from re-binding experiments and Langmuir adsorption isotherms are evaluated and discussed. The conclusions and possible future work are outlined in chapter 6.

# CHAPTER 2

# THEORETICAL BACKGROUND

## 2.1 Introduction

The relevant aspects pertinent as background information are discussed in this chapter. The chapter begins with an overview of conducting polymers; the aim is to describe conducting polymers (CPs) in a simplified manner that highlights the salient characteristics of this class of materials. The discussion narrows down to polyaniline which is the polymer chosen in this study because of its ease and low cost of synthesis as well as stability when compared to other conducting polymers. The band theory, conduction mechanism and electrical conductivity of conjugated polymers are discussed in subsequent sections. The final part of this chapter provides a brief summary of application of conducting polymers especially in chemical sensors.

## 2.2 Conducting Polymers

The notion that plastics could conduct electricity never came to the attention of scientists until their accidental discovery in 1977 [4]. These special plastics called conducting polymers have attracted a lot of attention in the research and scientific community because of their possible and promising applications [5, 6]. The combination of their polymeric nature and electronic conductivity put them in a favourable position which conventional inorganic materials are not with regard to applications and products. Conducting polymers offer new applications in areas such as molecular electronics, electronic drug delivery, large screen displays, biosensors, chemical sensors, photovoltaics and tunable electromagnetic interference shielding[6].

Conducting polymers are mainly organic compounds that have an extended π-orbital system, through which electrons can move from one end of the polymer to the other [7]. The most prominent types of conjugated polymers are polyaniline, polypyrrole, and polyacetylene (see Table 1) and derivatives thereof, which have been studied intensely primarily due to their intrinsic conductivity. Others include polythiophenes,

polyphenylenes, polyfluorenes, poly-(arylenevinylene)s and poly(phenyleneethynylene)s which have also been studied extensively due to their electro, optical and photoluminescent properties. Table 1 gives examples of names and structures of common conducting polymers.

**Table 1: Names and structures of some common conducting polymers [7].**

| Conducting Polymer | Structure |
|---|---|
| Polyacetylene | 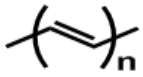 |
| Polyparaphenylene | 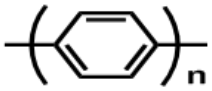 |
| Polyparaphenylene vinylene | 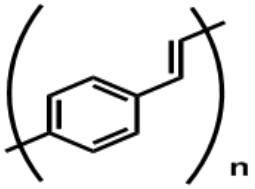 |
| Polyazulene | 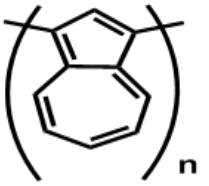 |
| Polyaniline | 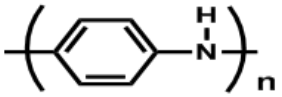 |
| Polyparaphenylene sulfide | 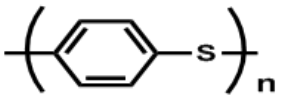 |
| Polypyrrole | 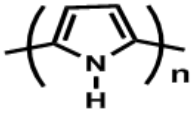 |
| Polythiophene | 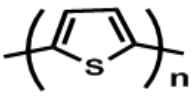 |
| Polycarbazole | 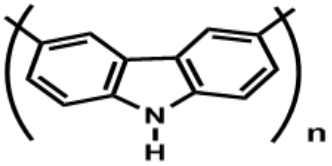 |
| Poly(1,8-diaminonaphthalene) | 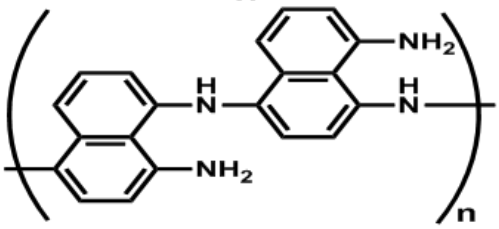 |

### 2.2.1 Electronics of conducting polymers

Conducting polymers are extensively conjugated molecules that have alternating single and double bonds. In these molecules, electrons are able to move from one end of the polymer to the other through the extended $\pi$-orbital system [7]. CPs are known to be either semiconductors or conductors, this is related to how bands and shells of electrons form within a compound. Thus, in order to explain the mechanism as well as the electronic properties of CPs, the band theory is employed. The theory originates from the formation of energy bands in polymer materials from discrete orbital energy levels found in single atom systems.

### 2.2.2 The band theory as a function of application of quantum theory

The physical chemistry approach to explanation of band theory is to relate it to the quantum theory of atomic structures. The first major success of quantum theory was its explanation of atomic spectra, particularly that of the simplest atom, hydrogen [8]. Quantum mechanics introduced an important concept which explained that atoms could only occupy well-defined energy states and for isolated atoms the energy states were very sharp [8]. The resulting spectral emission lines correlated to electrons jumping from one allowed energy state to another, and this gave rise to correspondingly narrow line widths [8]. In a crystalline solid, atoms cannot be viewed as separate entities, because they are in close proximity with one another, and are chemically bonded to their nearest neighbour [9]. This leads to the concept that an electron on an atom is affected by the electric field due to electrons on other atoms. Thus, the nature of the chemical bond formed implies that electrons on close-neighbour atoms are able to exchange positions with one another, causing the broadening of sharp atomic energy states into energy ‘bands’ in the solid [9]. This can be illustrated using an example in Figure 2, that depicts 3p and 3s electron shells for a single metallic atom in the third period of the periodic table that overlap to become bands that overlap in energy [9]. The association of these bands is no longer solely with single atoms but rather with crystal as a whole. In other words, electrons may appear with equal probability on atoms anywhere else in the crystal.

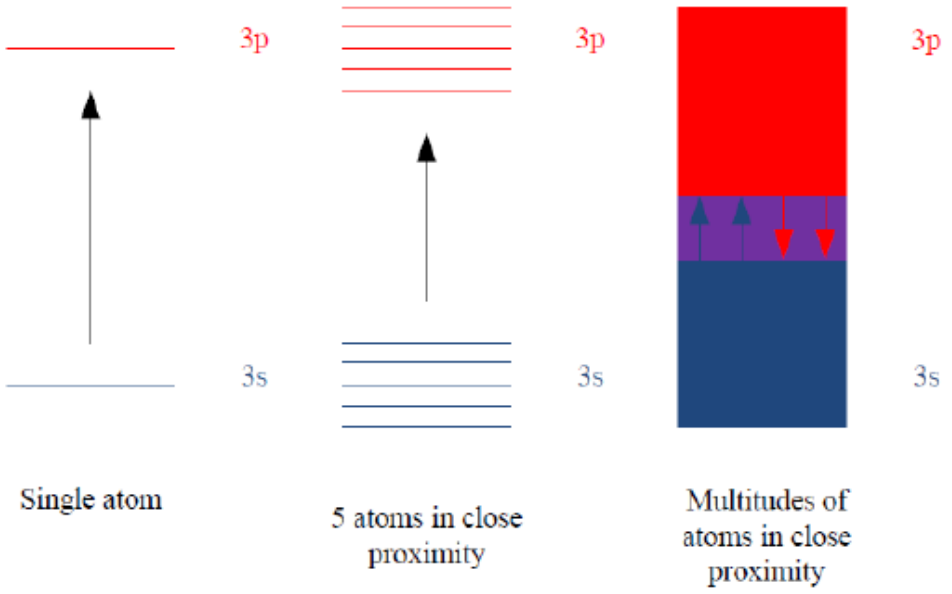


**Figure 2: The formation of bands in a conducting solid in the 3rd period and overlap between the valence and conduction bands[9].**

### 2.2.3 The band theory as a function of application of molecular orbital theory

The chemical approach to band theory is to relate it to molecular orbital theory. In molecular orbital theory, using H(1) and H(2) hydrogen atoms as an example (Figure 3), an atomic orbital from H(1) atom can overlap with an atomic orbital of H(2) atom, resulting in the formation of two molecular orbitals known as the bonding and antibonding molecular orbitals [9]. These are delocalized over both atoms, and the bonding molecular orbital possess lower energy than the H(1) and H(2) atomic orbital, while the antibonding molecular orbital has higher energy.

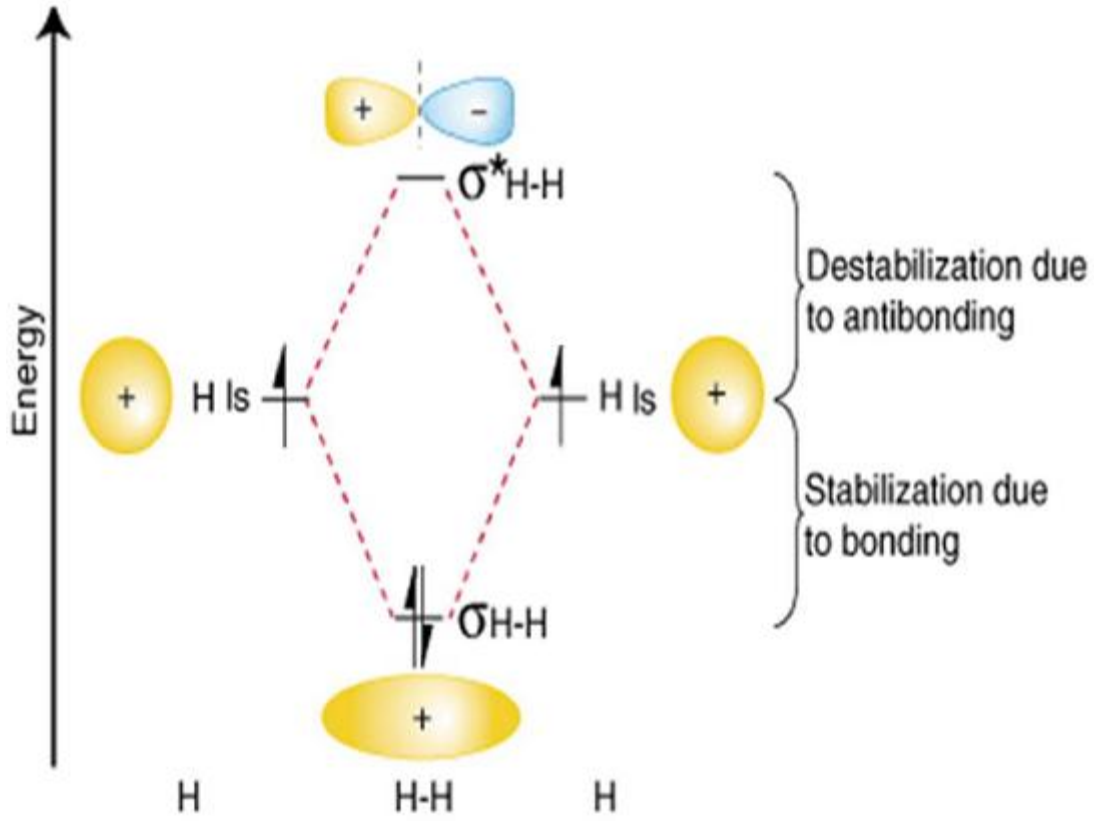


**Figure 3: Molecular orbitals in a diatomic molecule [10].**

The energy band that results from the bonding orbitals of a molecule is known as the valence band, while the conduction band is as a result of the antibonding orbitals of the molecule as illustrated in Figure 3.The valence band (VB) represents the highest occupied molecular orbital (HOMO) and the conduction band (CB) represents the lowest unoccupied molecular orbital (LUMO)[10]. The gap between the highest filled energy level and lowest unfilled energy level is called band gap (Eg). This band gap represents a range of energies which is not available to electrons. This gap is known variously as 'the fundamental energy gap', the 'band gap', the 'energy gap', or the 'forbidden gap' [8]. The level of electrons in a system which is reached at absolute zero is called the Fermi level (Fg) [11]. Combining the concepts explained in both atomic and molecular orbital theory, the electronic properties of metals, semiconductors, and insulators can be differentiated with reference to the energy band gap as shown in Figure 4. The conducting properties of different types of materials can be explained using the band gap model. Materials are conducting, semi-conducting or insulators depending on the extent of energy difference between

the valence and conduction bands (Figure 4). An understanding of the band structure of CPs is important for one to be able to appreciate why CPs are described by the same treatment as inorganic semiconductors.

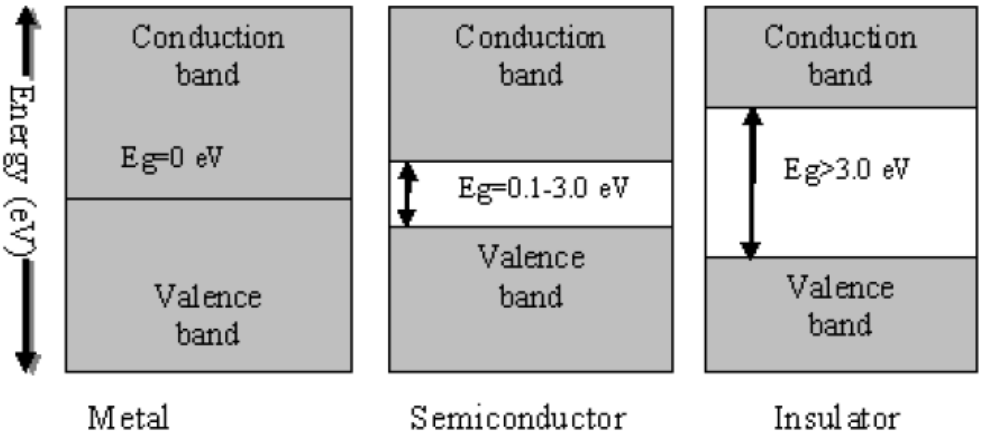


**Figure 4: Energy band diagram demonstrating band gaps [8].**

## 2.2.4 Charge transfer in conducting polymers

The general band theory described above provides a foundation in the charge transport system in conducting polymers. In CPs, electronic charge transport requires motion of charge along the polymer backbone. It has been demonstrated that in order to allow the formation of delocalized electronic states, CPs molecular arrangement must be conjugated [12]. The delocalization of the electronic states relies on the resonance stabilized structure of the polymer. The size of the energy band gap depends on the extent of delocalization and the alternation of double and single bonds [10]. Moreover the size of the energy band gap will determine whether the CP is metal, semiconductor or insulator [10].

The conductivity of certain organic polymers can be raised to metallic levels by chemical or electrochemical `p-doping' (oxidation), or `n-doping' (reduction).The doping of an organic polymer to achieve certain metallic properties is phenomenologically similar to the doping of a classical inorganic semiconductor in that very large increases in conductivity are observed when the material takes up

very small amounts of certain chemical species. However, mechanistically it is different in that the doping of an organic polymer involves simply the partial oxidation or reduction of the polymer, each oxidation state exhibiting its own characteristic reduction potential. The dopant ion incorporated may be derived from the chemical dopant species or it may be completely unrelated to it. The conjugated polymers in their undoped state are semiconductors or insulators because they have energy gap which is greater than 2 eV. This energy gap is too great for thermally activated conduction. A semi conductor can be categorised as intrinsic or extrinsic depending on whether it is pure or doped [13].

In undoped form, semiconductors are intrinsically conducting while the doped semiconductors are extrinsically conducting. In reverse, doped polymers are often referred to as "intrinsically conducting polymers". This is to distinguish them from polymers which acquire conductivity by loading with conducting particles such metal flakes, carbon black or fibers of stainless steel. The intrinsically conducting polymers (ICPs), more commonly known as "synthetic metals" are organic polymers which possess the mechanical properties and processability of conventional polymers, as well as unique electrical, electronic, magnetic, and optical properties of metals [14]. Conducting polymers can exist in nonconductive form (non-doped polymer) and conductive form (doped polymer) [15].The "classical" method of "doping" involves redox doping, i.e., chemical or electrochemical partial oxidation ("p-doping"), or partial reduction ("n-doping") of the conjugate polymer backbone [15]

## 2.2.5 Conductivity in Polyaniline

Polyaniline is known as a mixed oxidation state polymer composed of reduced benzoid units and oxidized quinoid units [16]. As a mixed oxidation state polymer, PANI's average oxidation state is denoted as 1-y whereby the value of y determines the existence of each of the three distinct PANI oxidation states [16, 17] as shown in Figure 5. Thus, PANI exists as fully reduced leucoemeraldine (LE) where 1-y = 0, half oxidized emeraldine base (EB) where 1-y = 0.5 and fully oxidized pernigraniline (PE) where 1-y = 1 [16]. The EB is regarded as the most useful form of polyaniline

due to its high stability at room temperature, it is composed of two benzoid units and one quinoid unit that alternate and it has known semiconductor properties [18].

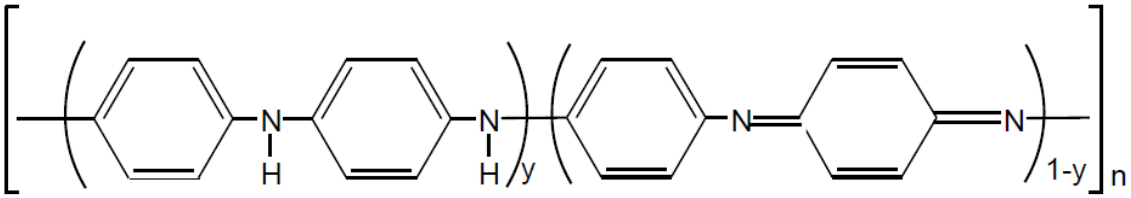


**Figure 5: Different oxidation states of polyaniline (y = 1: leucoemeraldine, y = 0.5: emeraldine and y=0: pernigraniline [19].**

The conductivity of PANI varies with the extent of oxidation (variation in the number of electrons) and the degree of protonation (variation in the number of protons). Among the various oxidation states that PANI can exist in, the one that can be doped to a highly conductive state is the moderately oxidized emeraldine base [19]. This form of PANI has a structure which consists of equal proportions of amines (–NH–) and imine (=N–) sites. Through protonic acid doping, imine sites are protonated by acids HA to the bipolaron (dication salt) form [20]. The bipolaron then undergoes a further rearrangement to form the delocalized polaron lattice which is a polysemiquinone radical-cation salt as shown in Figure 6. The resulting emeraldine salt has conductivity on a semiconductor level of the order of 100 S $cm^{-1}$.This is many orders of magnitude higher than that of common polymers ($<10^{-9}$ S $cm^{-1}$) but lower than that of typical metals ($>10^{4}$ S $cm^{-1}$) [21]. Only 1% of the charge carriers which are available in the ES salt actually contribute to its observed conductivity. If all the available charge carriers were to contribute, the resulting conductivity at room temperature would be approximately $10^{5}$ S $cm^{-1}$, which is comparable to that of copper [22]. In general, maximum conductivity is achieved when PANI is in the emeraldine salt state, in this state the polaron states overlap to form mid-gap bands [23].The electrons are thermally promoted at ambient temperatures to the unfilled bands, which permit conduction.

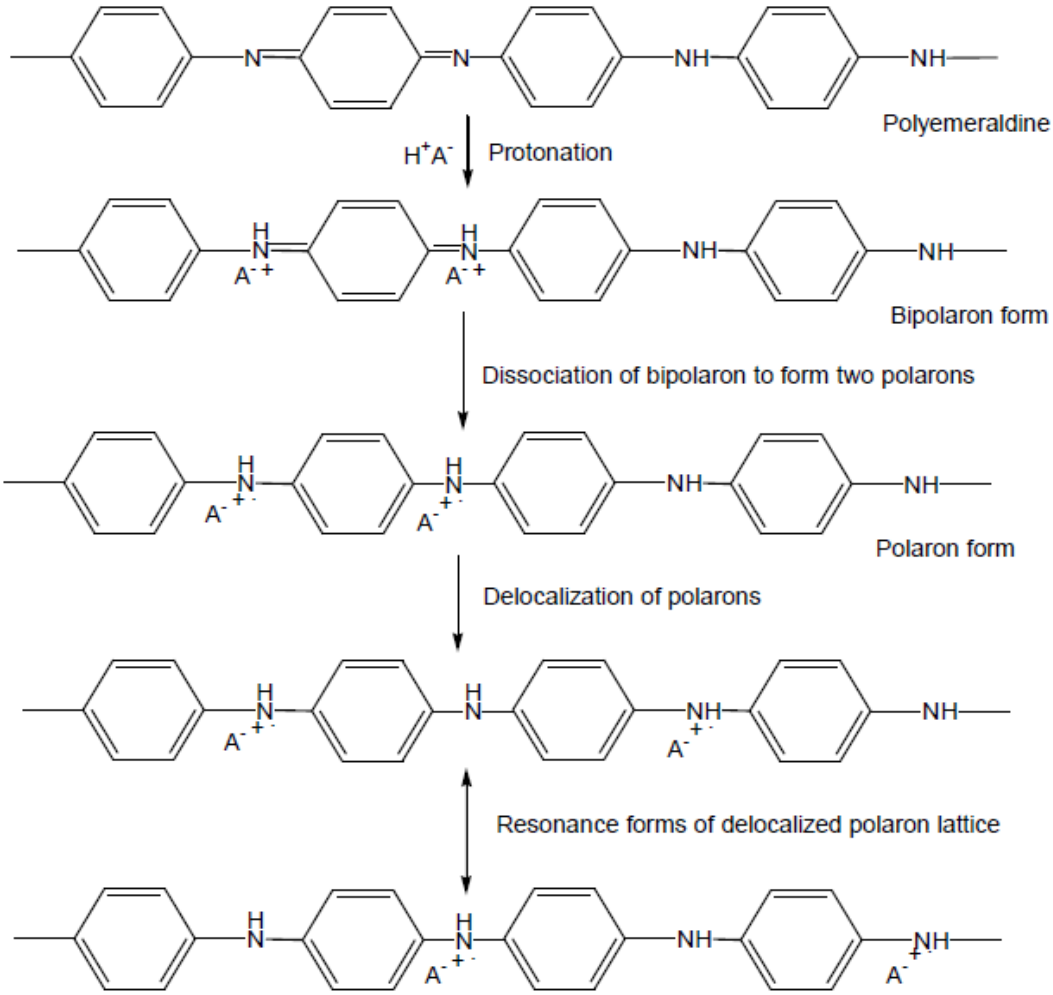


**Figure 6: The doping of EB with protons to form the conducting emeraldine salt (PANI/HA) form of polyaniline (a polaron lattice) [24].**

## 2.2.6 Application of Conducting Polymers

Many types of analytical applications of the conducting polymers have been reported since their discovery. Conjugated polymers are widely investigated for applications relying on their conductivity, photo- or electroluminescence, or light-induced charge generation. This includes applications such as light-emitting devices and displays, photovoltaics [25] or chemical sensors [26] of variable complexity concerning their structure and function [14]. During the last two decades, conducting polymers have emerged as one of the most interesting materials for the fabrication of electrochemical sensors [7]. The great advantage of conducting polymer based sensors over other available devices is that the conducting polymers have the potential to exhibit improved response properties and are sensitive to small perturbations. Previously, inert (non- conducting) polymers were being used only to provide mechanical strength, but recently conducting polymers are also used to improve the sensitivity of the sensors due to their electrical conductivity. Amongst many analytical techniques available, chemical sensor development has made one of the largest strides in the development of analytical tools.

### 2.2.6.1 Chemical Sensor

A chemical sensor is a device that transforms chemical information, ranging from the concentration of a specific sample component to total composition analysis, into an analytically useful signal [27]. The chemical information may originate from a chemical reaction with the analyte or from change in physical properties of the system being investigated. Chemical sensors contain two basic functional units: a receptor part and a transducer part [28]. Some sensors may include a separator, for example, a membrane. In the ***receptor*** part of a sensor the chemical information is transformed into a form of energy which may be measured by the transducer. The ***transducer*** part is a device capable of transforming the energy carrying the chemical information about the sample into a useful analytical signal (Figure 7) [27]. The receptor part of chemical sensors may be based upon various principles:

(a) Physical: No chemical reaction takes place. Typical examples are those based upon measurement of absorbance, refractive index, conductivity, temperature or mass change.

(b) Chemical: Chemical reaction occurs with participation of the analyte that gives rise to the analytical signal.

(c) Biochemical: A biochemical process is the source of the analytical signal. Typical examples are microbial potentiometric sensors or immunosensors. They may be regarded as a subgroup of the chemical ones. Such sensors are called ***biosensors.***

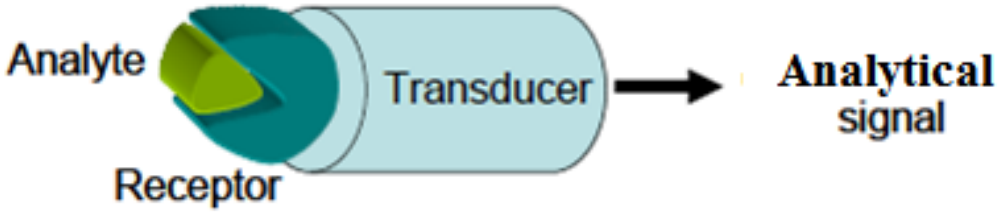


**Figure 7: Schematic presentation of a chemical sensor.**

## 2.3 Molecular Imprinting

Molecular imprinting is a process where functional monomers and crosslinkers are copolymerised in the presence of a template molecule [29]. It is assumed that functional monomers form a complex with the template molecule prior to polymerisation. After the polymerisation process, the functional groups are held in position by the highly cross linked polymeric structure. The removal of the template molecules from the cross linked matrix forms binding sites that are complementary in size and shape to the template. The MIP obtained can subsequently recognise and bind the template molecules. Molecularly imprinted polymers (MIPs) are synthesized either by covalent approach, non-covalent approach or semi covalent approach [30].

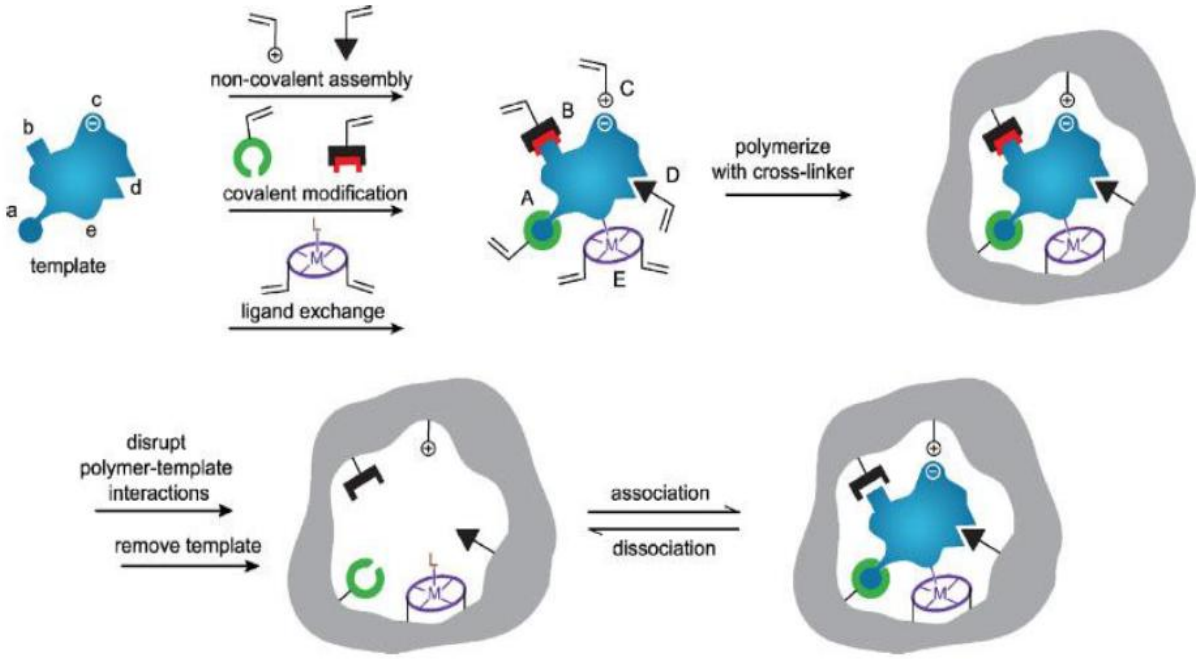


**Figure 8: Schematic representation of molecular imprinting. The template and the functional monomers may interact by:(A) reversible covalent bonds, (B) covalently attached polymerisable binding groups, subsequently activated for non-covalent interaction by template cleavage, (C) electrostatic interactions, (D) hydrophobic or van dar waals interactions, (E) metal-ion mediated interactions. Each one of these is established with complementary functional groups or structural elements of the template (a-e), respectively. Adapted from reference [30].**

As Figure 8 shows, the synthesis of molecularly imprinted polymers involves one or more types of monomer, which possess functional groups capable of interacting with the target molecule (template), either covalently or through non-covalent interactions. The reaction mixture includes also a cross-linker agent and a porogenic solvent. After mixing, the polymerisation system is allowed to cure thermally or using UV light resulting in a highly cross-linked polymer with a porous structure [30]. After this step, the template is usually removed from the imprinted polymer by washing with solvent or through a combination of chemical treatments and washing steps. This leaves behind binding sites that are both spatially and chemically complementary to the template molecules, and capable of rebinding the template [30].

## 2.3.1 Molecular imprinting approaches

Three main kinds of molecular imprinting strategies can be identified. They are all classified according to the nature of the bonds established between the template and the functional monomers, and in particular they are indicated as covalent, semi-covalent and non-covalent approaches.

### 2.3.1.1 Covalent imprinting

Covalent imprinting approach was pioneered by Wulff and colleagues [31] and it involves the covalent modification of the template, which is chemically bound to the functional monomers in a reversible way. This modification is then followed by the polymerisation step, during which the template is still covalently connected to the monomer, now polymerised. Finally, the template is cleaved through a mild chemical reaction (e.g. hydrolysis or reduction), leaving behind the binding cavities. This approach shows very important advantages, such as that due to the strong interaction which occurs between the template and the functional monomer, it usually leads to binding sites that are quite homogeneous [32]. However, both the removal of the chemically bound template and its subsequent rebinding are not simple, because they involve the disruption and the re-establishment of covalent interactions, which in turn make the kinetics of these processes really slow. This latter point has to be considered, especially in the case of separation applications, in which the presence of a fast rebinding kinetics is important [33]. Moreover, the prior derivatisation of the template is not easy with this approach, and is dependent on the chemical nature and the available functional groups of the template [34].

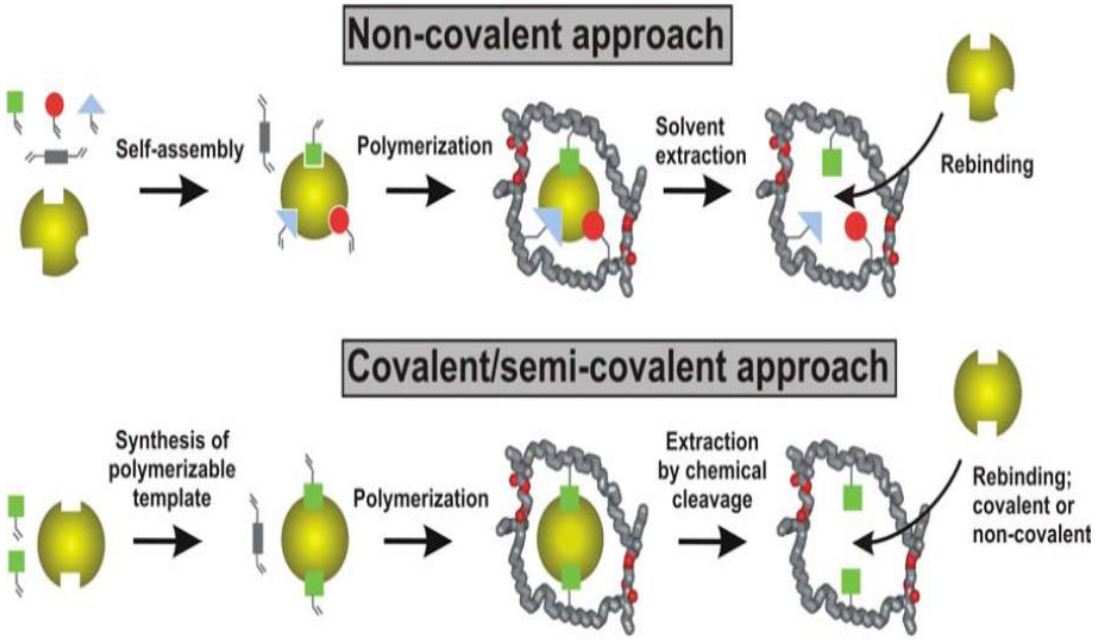


**Figure 9: Schematic representation of covalent, semi-covalent and non-covalent approach (adapted from reference [2].**

## 2.3.1.2 Semi-covalent imprinting

A variation of the above-mentioned method has been developed by Sellergren and Andersson [35].The process consists of a polymerisation step that involves binding the template, usually via an ester bond, while the second step (rebinding process) takes place through non-covalent interactions. This strategy is a modification of the covalent and non covalent approach. The template is typically washed out via hydrolysis from a crosslinked polymer matrix

## 2.3.1.3 Non-covalent imprinting

Klaus Mosbach and co workers [36] promoted the non covalent imprinting strategy which is still the most frequently used MIP technique in developing artificial receptors. The monomer-template complex is formed by non- covalent interactions. Since removing the template molecules does not involve breaking any bond, it is usually straightforward and can be achieved by washing or evaporation. It exploits several kinds of non-covalent interactions between the template and the monomers; such as hydrogen bonding, electrostatic and hydrophobic interactions (for example

van der Waals forces). However, this approach is far from being free from drawbacks, since it often leads to a broad distribution of heterogeneous binding sites [37].

## 2.3.2 Emulsion Polymerisation

Emulsion polymerization is one of the fastest methods for nanoparticle preparation and is readily scalable. The method is classified into two categories, based on the use of an organic or aqueous continuous phase. The continuous organic phase methodology involves the dispersion of monomer into an emulsion or inverse microemulsion, or into a material in which the monomer is not soluble (non solvent) [38]. Emulsion polymerization is the commonest way of forming polymer latexes; in the simplest system, the ingredients comprise water, a monomer of low water solubility (e.g. styrene), water-soluble initiator (e.g. persulfate) and surfactant (latexes can also be synthesized without added surfactant and/or initiator, but these are not common) [39]. A new phase quickly forms: a polymer colloid, comprising a discrete phase of colloidally stable latex particles, dispersed in an aqueous continuous phase. Virtually all polymerization occurs within these nanoreactors [39].

Ruckenstein and co workers [40] employed inverted emulsion polymerisation for the synthesis of PANI composites using an isooctane-toluene mixture and water to form the emulsion employing ammonium persulfate as the oxidant. Inverse emulsion polymerisation consists of an aqueous solution of a monomer which is emulsified in a non polar organic solvent, for example chloroform, and the polymerisation is initiated with an oil-soluble initiator. The other strategy reported for fabrication of PANI NPs is micro-emulsion polymerisation. Jang and co workers [41] reported fabrication of monodisperse and nanometer-sized PANI spheres as small as 4nm using micro-emulsion polymerisation. This technique allows particles to transfer into spherical aggregates through the surfactant template. There are two reasons for using the surfactant in the polymerisation. One is the creation of a micro-reactor vessel via micelle formation, where monomer is restricted in a localised environment originated from encapsulation by the surfactant (Figure 10). The second reason is to improve the physical properties of polymers such as conductivity, stability, solubility in organic solvents and processibility.

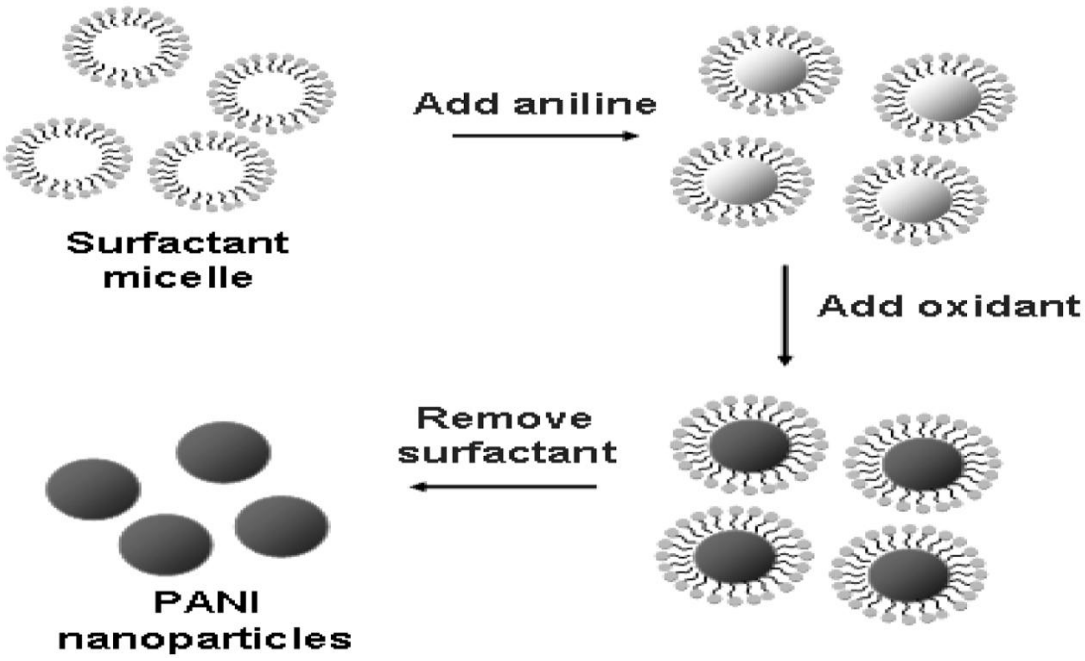


**Figure 10: Schematic representation for the surfactant templating of PANI nanoparticles (adapted from reference [38].**

## 2.3.2.1 Advantages of Nano MIPs

Emulsion polymerisation has been used to prepare molecularly imprinted nanoparticles [42]. Molecularly imprinted nanoparticles have several advantages over their bulk counterparts because among other things, MIP NPs have greater total surface area per weight unit of polymer thus increasing the rate of interaction between the template and MIP. Apart from that, the solubility of polymers greatly improves when they are synthesised in their nano size. Also there is better control of manufacturing process using chemical reactors hence the size and shape of the synthesised particles can be easily controlled. Furthermore, imprinted cavities are more easily accessible to the template, which improves binding kinetics and facilitates the template removal process, thus enhancing their overall performance. This is clarified in the scheme elaborated by Gao and co-workers [43] (Figure 11).

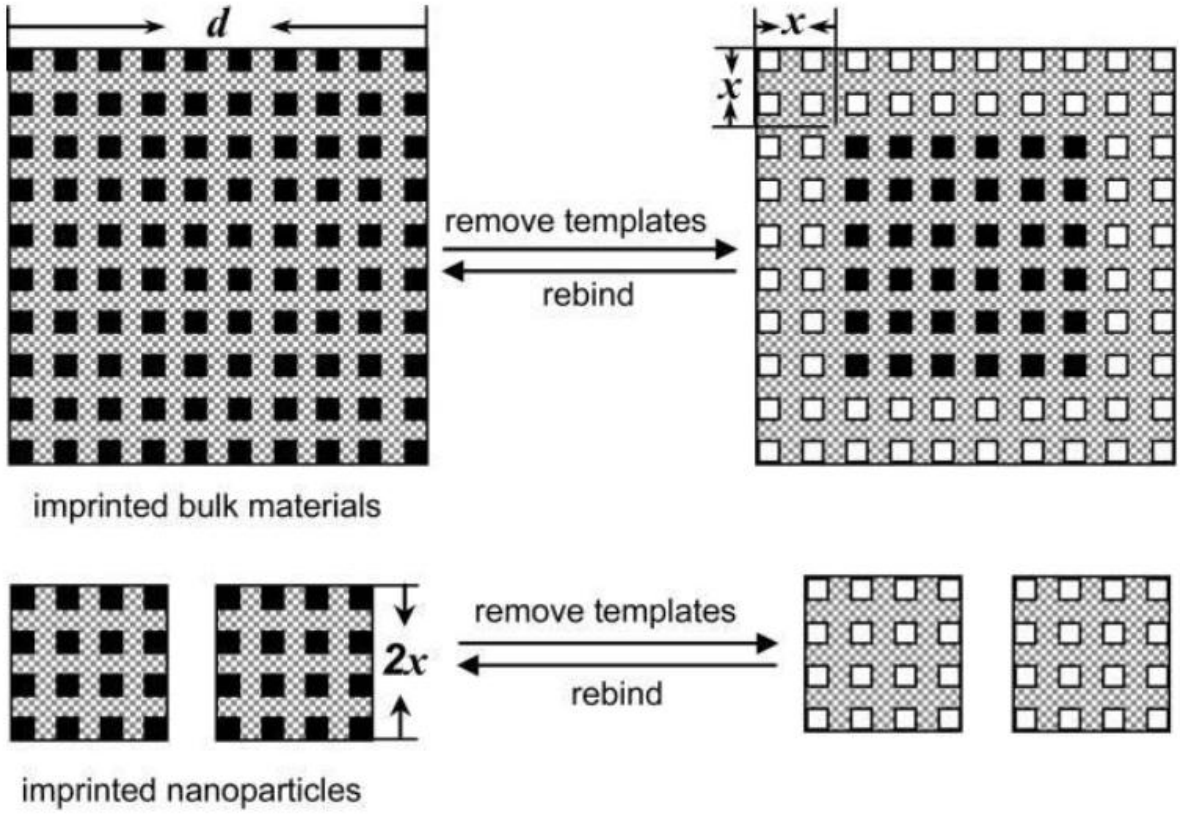


**Figure 11: Schematic representation of the distribution of effective binding sites in the imprinted bulk materials and MIP NPs before and after the template removal step. Black squares represent template/analyte imprinted onto polymer matrix, white squares represent template/analyte extracted from polymer matrix. Adapted from reference [43].**

According to this model, for a bulk imprinted polymer with a size d, in Figure 11, above, only the templates which are within *x* nm from the surface may be removed. If the imprinted materials are prepared as NPs with a scale of *2x* nm, all the sites may be completely accessible and effective for removing the template and then for rebinding the template molecules. Table 2 below shows comparison of properties of bulk MIPs and MIP NPs.

**Table 2: Comparison of properties of bulk MIPs and MIP NPs [44].**

| Bulk MIPs | MIP NPs |
|---|---|
| Broad distribution of binding sites with varying affinity, high level of non specific binding | Similar affinity for all binding sites, 1-2 per particle, 2-3 orders of magnitudes difference between specific and non specific binding |
| Affinity in the range $10^{-9}$ - $10^{-3}$ M depending on template | Affinity in the range $10^{-10}$ - $10^{-6}$ M, possibility of using affinity chromatography for the fractionation of high-performance NPs |
| Insoluble material difficult to process | Soluble NPs which can be treated as standard reagents |
| Substantial batch to batch variability | Better control of manufacturing process using chemical reactors |
| Possibility of template leaking from polymer | Traces of template can be relatively easily removed using dialysis or affinity separation |
| Limited prospects for in vivo applications | MIP NPs with biological activity can be produced |

# CHAPTER 3

# LITERATURE REVIEW

## 3.1 Introduction

This chapter reviews literature on the use of emulsion polymerisation in the preparation of molecularly imprinted nanoparticles. The study of molecularly imprinted nanoparticles is "relatively" new, the literature base, although rapidly expanding is still relatively small. Most of the literature reviewed in this chapter is the work of the pioneers and highly acclaimed “researchers” in this field notably Vaihinger D, Piletsky S.A, Turner A.P.F, Whitcombe M.J, Alexander C, Carboni D, Ciardelli G, Yoshimatsu K, and many more .The discussion is intended to highlight current efforts by several researchers in nano-MIP fabrication and also their application in pesticide analysis.

## 3.2 Preparation of Molecularly Imprinted Nanoparticles by emulsion polymerisation

The application of emulsion polymerisation to obtain MIP NPs is quite recent, and it was first performed by Vaihinger and co-workers [45], who used it to obtain NPs imprinted with L- or D-Boc-Phenylalanine anilid (BFA). Emulsion polymerisation is usually carried out by producing an O/W emulsion in which monomer, cross-linker and template are in the disperse phase, while the initiator is in the continuous aqueous phase. The polymerisation reaction then occurs in micelles stabilised by a suitable surfactant. In the work of Vaihinger and colleagues [45], the oil phase was composed of MAA as functional monomer and EGDMA as cross-linker, used in different molar ratios in order to study their effect on the particle size. This phase was then mixed by vigorous stirring with the aqueous continuous phase composed of surfactant SDS dissolved in water. The mixture was then sonicated and polymerised at 80 °C for 16 hrs. A very high conversion rate (about 98%) of the nanodroplets into MIP NPs was obtained. Moreover, due the use of the hydrophobic initiator AMBN, the polymerisation occurred just in the droplets. The MIP NPs produced also exhibited very good enantio-selectivity, in particular when the monomer-to-cross-

linker molar ratio was 1:4. MIP NPs imprinted with L-BFA bound this template 10-fold more efficiently than they bound the D-enantiomer. They also had very good affinity, since NIP NPs bound the template 4-fold less than the MIP. However, these rebinding properties were exhibited only when the amount of template was above 5 μmol. Moreover, despite the particles obtained being regularly spherical, their polydispersity was quite pronounced. The diameters ranged between 50 and 300 nm (Figure 12)

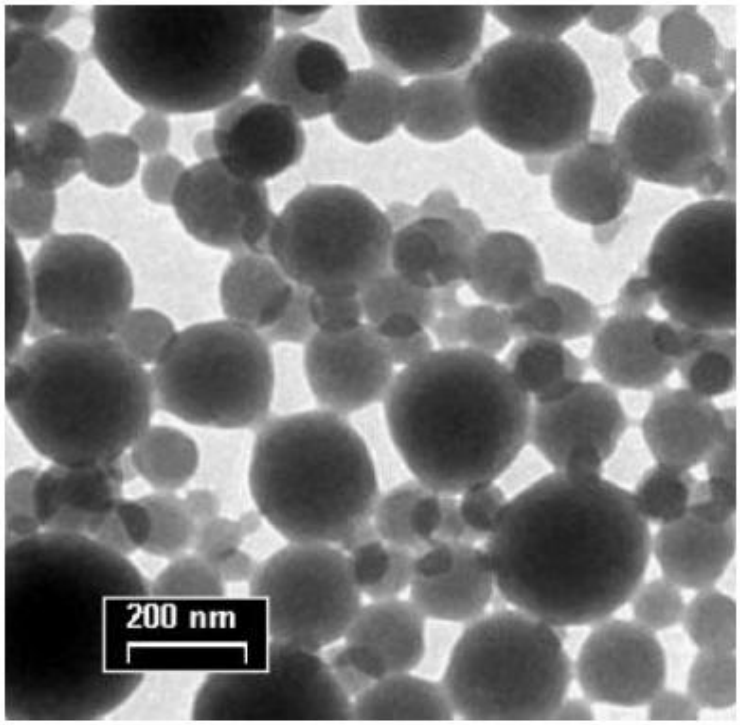


**Figure 12: Transmission electron microscopy (TEM) image of MIP NPs produced through mini-emulsion polymerisation by Vaihinger et al [45].**

Recently Curcio and his group [46] prepared MIP NPs imprinted with glucopyranoside using the mini-emulsion polymerisation technique. They exploited a semi-covalent imprinting technique instead of a non-covalent one in order to force the template to be located on the surface of the MIP NPs. For this purpose, a polymerisable surfactant template was synthesised, with four acrylic ester groups and a lipophilic chain with a polar sulphonated head. This compound was dissolved in styrene (St), chosen as functional monomer, and DVB. AMBN and hexadecane were subsequently added and solution mixed with an aqueous solution of SDS under ultrasonication. The mini-emulsion obtained was thermally polymerised at 80 °C for

20 hours, after which the template was removed by alkaline hydrolysis. MIP NPs exhibited good rebinding capacity in comparison with non-imprinted ones, as well as very good selectivity for glucopyranoside rather than galactopyranoside ($\alpha = 6.5$). Also the rebinding kinetics was quite fast, taking only 5 hours to reach the equilibrium, while MIPs prepared by bulk polymerisation usually requires 24 to 48 hours. According to the Scatchard analysis [37], two classes of binding sites with low ($K_D = 5780 \times 10^{-6}$ M) and high affinity ($K_D = 439 \times 10^{-6}$ M) had been created. However, the use of a semi-covalent imprinting approach did not allow removing the entire template from MIP NPs. Moreover, the synthesised MIP NPs did not exhibit a homogeneous size distribution when analysed by TEM (Figure 13).

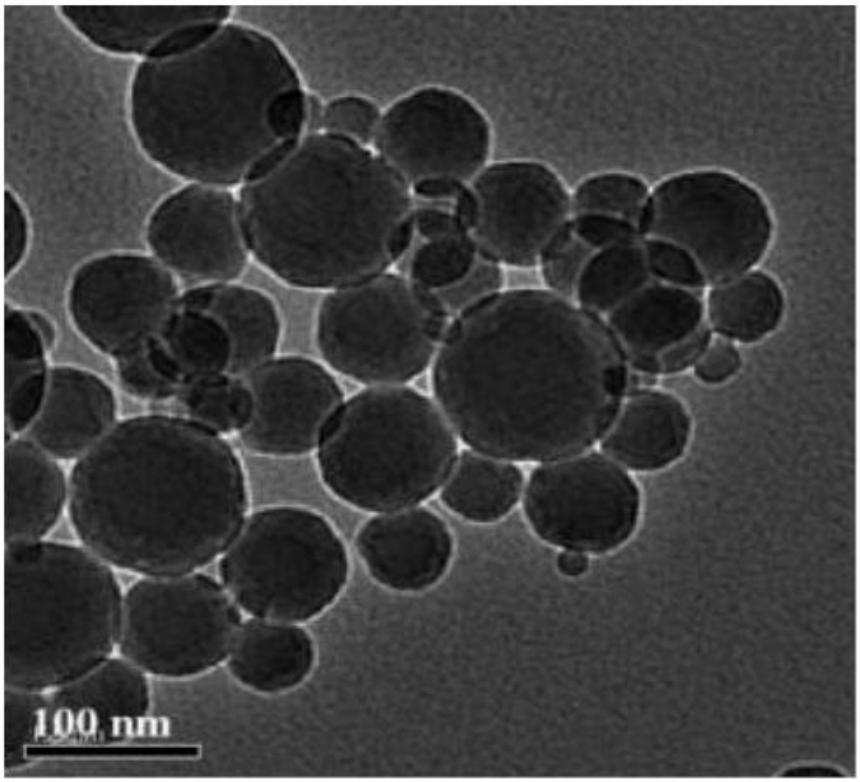


**Figure 13: TEM image MIP NPs synthesized by Curcio et al [46].**

Another group, Zeng and co-workers [47], very recently used a similar approach to obtain MIP NPs imprinted with a small hydrophilic peptide, GFP-9. They used an inverse micro-emulsion polymerisation, which involves creation of nanodroplets of an aqueous solution of monomers dispersed in an organic continuous phase. Also in this case, a surfactant was used to stabilise the droplets. The group used GFP-9

peptides coupled with fatty acid chains of different lengths (5, 13 and 15 carbon atoms) as a template. The polymerisation process was performed by dissolving in water AAm and N, N'-ethylenebisacrylamide, chosen respectively as monomer and cross-linker. This solution was then dispersed in the oil phase containing surfactants bis(2-ethylhexyl)sulfosuccinate sodium salt and Brij 30, dissolved in hexane. The modified peptides were then added and the mixture vigorously stirred to form the micro-emulsion. Finally, the polymerisation was started by adding APS and TMED then out for 2 hrs. Very small MIP NPs were obtained, about 28 nm in diameter and spherical in shape. Moreover, MIP NPs imprinted with the peptides coupled to acid chains of 13 and 15 carbon atoms exhibited a very strong affinity for the template and good specificity. The calculated $K_D$ ranged between 90 and 900 nM. However, MIP NPs imprinted with the template coupled to the shortest fatty acid chain did not exhibit any relevant imprinting effect. Probably the carbon chain (C5) was too short to successfully locate the templates onto the surface of the aqueous nanodroplets. The affinities of the binding sites were not distributed and only a small amount of high-affinity sites had been created. In addition the yields were not very high (50% w/w).

Dvorakova and co-workers [48] recently proposed a non-aqueous mini-emulsion imprinting polymerisation approach. This approach attempts to overcome the presence of water which characterises and disrupts the majority of mini-emulsion imprinting polymerisation process. It involves the use of a non-ionic, polymeric emulsifier, polyisoprene-block-poly(methyl methacrylate) co-polymer rather than a classic surfactant, and *n*-hexane and DMF respectively as external and internal phase of the emulsion. The authors used MAA and EGDMA as monomer and cross-linker with propranolol as template. These compounds were dispersed in DMF and then emulsified with the external phase containing the co-polymer through ultrasonication. The mini-emulsion was then polymerised thermally at 40 °C for 24 hrs after the addition of 2,2'-azobis(2,4-dymethylvaleronitrile) as initiator. Monodisperse MIP NPs of 100-120 nm in diameter were obtained. Predictably, both an increase in the amount of emulsifier and a decrease in the volume of internal phase resulted in a decrease in the NPs diameter. MIP NPs exhibited an evident imprinting effect when compared to their non imprinted polymer (NIP) counterparts,

up to 30% mol of specific template rebinding, with a specific $K_A$ of $1.68 \times 10^6$ $M^{-1}$ (about 2 orders of magnitude higher than the $K_A$ calculated for the NIP NPs).

## 3.3 Molecularly imprinted polymers in pesticide analysis

The following section outlines current efforts by several researchers in the use of conducting polymers in pesticide analysis. This review indicates the significant results that have been obtained.

Seyed M and co-workers [49] investigated the use of molecularly imprinted PANI to recognise chlorpyrofos and diazinon. The researchers prepared a chemical sensor based on molecularly imprinted polyaniline to recognise agricultural pesticides chlorpyrofos and diazinon. In that study, PANI was prepared by the traditional bulk polymerisation and films were developed from the prepared PANI. The sensing behaviour of molecularly imprinted polymer powder based on polyaniline was conducted as well as the spectral analysis. The conductivity measurements were taken using four point probe. Furthermore, it was found that the preparation process of molecular imprinting polymer and sensing properties done with this method for compounds such as diazinon and chlorpyrifos, show that the molecular imprinted surface in combination with the conductometric method is a useful approach for the sensing applications.

Furthermore, Tamayo F.G and co-workers [50] prepared three different molecularly imprinted polymers (MIPs) by precipitation polymerisation using linuron (LIN) or isoproturon (IPN) (phenylurea herbicides) as templates and methacrylic acid (MAA) or trifluormethacrylic acid (TFMAA) as functional monomers. According to the obtained results, the authors concluded that precipitation polymerisation was a powerful strategy for the preparation of MIPs with improved characteristics. The degree of homogeneity obtained, compared to that reported in MIPs prepared using the covalent approach, makes this polymerisation methodology a clear alternative to the traditional bulk polymerisation process. The influence of template during polymerisation prevents the attainment of imprinted beads. This in turn prevents its potential use in the preparation of stationary phases to be used in HPLC hence requiring further research.

In addition, Prasad and co-workers [51] report a new strategy to construct a potentiometric biomimetic sensor for direct, rapid and highly selective detection of atrazine. The stability, reusability and dynamic response time are analogous to conventional chemical sensors. The utility of the sensor was successfully tested for field monitoring of atrazine in ground waters. D´Agostino and co-workers [52] developed a potentiometric sensor for the herbicide atrazine based on a molecularly imprinted polymeric membrane. The membrane was formed directly at the end of a small teflon tube which was filled with a solution at constant composition, in contact with an internal reference electrode, as in a classical potentiometric cell for ion selective electrode. Atrazine is protonated, and as a consequence, positively charged in aqueous solution at sufficiently low pH. The combination of the positively charged species with the imprinted membrane produced a variation of the membrane charge.

In another report [53], an electropolymerized molecularly imprinted polymer was used as a selective receptor layer for the pyrethroid insecticide fenvalerate. A capacitive chemical sensor for fenvalerate based on an electropolymerized molecularly imprinted polymer as sensitive layer was developed. To test the selectivity of the sensor for fenvalerate, an interference test was performed, including common pyrethroid insecticides such as fenpropathrin, deltamethrin, alphamethrin and cypermethrin.

Furthermore, MIPs have been synthesized for detection of organophosphorus pesticides (OPPs).Three OPPs widely used in agriculture (diazinon, quinalphos and chlorpyrifos) were selected as target analytes. Mohd Marsin Sanagi and co-workers [54] synthesized an MIP based on O,O-diethyl-O-2- quinoxalinyl phosphorothioate (quinalphos) as a template for use in MIP-SPE sample enrichment of selected OPPs, namely quinalphos and two other OPPs with similar structure (diazinon and chlorpyrifos) in fruit samples prior to HPLC-UV analysis. In this study, various parameters affecting the extraction efficiency of the imprinted polymers were evaluated to optimize the selective preconcentration of OPPs from water samples. Under the optimized conditions, the developed MIP-SPE method showed excellent linearity in the range of 4 – 200 mg $L^{-1}$ with coefficient of determination ($r^2$) > 0.997 and good OPP recoveries of > 91%. Organophosphorous pesticides (OPPs) are one of the most common classes of pesticides involved in human poisoning because of the inhibition of acetyl-cholinesterase.

In contrast to these intense studies on the preparation of molecularly imprinted polymers from various functional monomers which have been reviewed extensively, preparation of MIPs from conjugated polymers nanoparticles have been relatively little addressed. It is clear from various works reviewed that preparation of MIPs from conjugated polymers nanoparticles and their properties in the bulk or thin films have not been extensively explored making necessary the study under consideration.

# CHAPTER 4

# EXPERIMENTAL TECHNIQUES

## 4.1 Introduction

In this chapter, the experimental techniques used in this work are explained. Firstly, the materials and apparatus used are listed. The sample preparation method is described followed by the film deposition technique which is the dip coating method. Structural characterisation techniques such as UV-VIS, FTIR, XRD as well as $H^1$ NMR are described. Morphology characterisation techniques such as AFM as well as SEM that were used are described in subsequent sections. Conductivity measurement that was performed to obtain I-V curves is described. Finally, the rebinding experiments on the synthesized molecularly imprinted polyaniline are described.

## 4.2 Materials

Aniline, aldrin, sodium lauryl sulphate, benzoyl peroxide, hydrochloric acid, acetone, ethanol and chloroform were all purchased from Sigma-Aldrich. All chemicals and solvents used within this work were used as received except for aniline which was double distilled prior to use. DDT was kindly donated by Dr Yvette Naudé (University of Pretoria). MilliQ double-distilled ultrapure water was used in all experiments.

## 4.3 Instrumentation

$^1$H-NMR studies were performed using a Bruker Avance 400 MHz NMR. Briefly the sample was analysed in liquid form using deuterated chloroform as solvent. The FT-IR spectra were recorded using KBr pellets on a Perkin Elmer Spectrum RXI FT-IR spectrometer. The sample was analysed in pellet form by mixing the sample with pre-dried KBr in 1:5 ratio. The sample was scanned over a range of 400 $cm^{-1}$– 4000 $cm^{-1}$. UV-VIS measurements were recorded using a Schimadzu 2000 UV- VIS spectrophotometer. The measurements were carried out on thins films of polyaniline on glass slides. AFM experiments were performed using a Bruker Dimension Icon

AFM in scanAsyst mode. The measurements were carried out on polyaniline thin films. SEM images of polyaniline thin films were recorded in a Zeiss Ultra plus scanning electron microscope and were carried out on polyaniline thin films prepared. X-ray diffraction pattern was obtained using an X'pert pro powder diffractometer (PANalytical Model, Iron filtered Co-Kα radiation with λ=1.789 Å at 50 kV, 30 mA).The sample in powder form was scanned over the required range of 10 - 70$^{o}$ for 2θ values. The phases were identified using X'Pert Highscore plus software. The conductivity measurement was by four point probe coupled to a source meter. Quantitative analysis of aldrin and 1,1,1-trichloro-2,2-bis(*p*-chlorophenyl)ethane (DDT) in solutions was performed by GC-TOFMS and one microlitre of solution was injected. Analyte separation was done using a LECO Pegasus 4D GC-TOFMS including an Agilent 7890 GC (LECO Africa (Pty) Ltd., Kempton Park, South Africa). The carrier gas, helium, was of ultra-high purity grade (Afrox, Gauteng, South Africa).

## 4.4 Sample Preparation

### 4.4.1 Preparation of Polyaniline nanoparticles

In the polymerisation reaction, 60 ml of 0.2 M benzoyl peroxide in chloroform was prepared and 1.44 g sodium lauryl sulphate in 50 ml of water (0.1 M) was added to it under constant stirring at room temperature to obtain a milky white emulsion. To this emulsion, 1 g (10.84 mmol) aniline monomers were added dropwise, followed by drop wise addition of dopant 90 ml (1.5 M HCl) over a period of 30 min. During the progress of the reaction, the colourless emulsion goes through colour changes from brown, purple, blue and finally green. The reaction was allowed to proceed for 24 hours with stirring. The organic phase containing colloidal particles was separated and washed repeatedly with deionised water to remove all surfactant. The dark green polyaniline in chloroform was then treated with anhydrous sodium sulphate to remove excess water. The viscous organic colloidal solution was then treated with excess acetone in order in order to break the emulsion and precipitate the polyaniline salt. It was then filtered, washed with acetone, and the dark green powder obtained was dried under vacuum at room temperature.

### 4.4.2 Preparation of Aldrin- Molecularly Imprinted Polymer

In the preparation of imprinted PANI NPs, 60 ml of 0.2 M benzoyl peroxide in chloroform was prepared and 1.44 g sodium lauryl sulphate in 50 ml of water (0.1 M) was added to it under constant stirring at room temperature to obtain a milky white emulsion. A mixture of 1 g (10.84 mmol) aniline monomers, 8 mg (0.0219 mmol) aldrin template in chloroform was taken and sonicated for 10 min to ensure that all material was dissolved. This solution was then slowly added to milky emulsion and stirred for 30 min. Dropwise addition of dopant, 90 ml (1.5 M HCl) followed over a period of 30 min. During the progress of the reaction, the colourless emulsion turns green. The reaction was allowed to proceed for 24 hours with stirring. The organic phase was separated and washed repeatedly with deionised water to remove all surfactant. The viscous organic solution was then treated with excess acetone in order to break the emulsion and precipitate the imprinted PANI NPs. It was filtered, washed with acetone to remove any unreacted aniline. The dark green powder obtained was dried under vacuum at room temperature. In order to extract the aldrin out of the polymer, the soxhlet extraction method was used in which the imprinted polymer was repeatedly washed with the dichloromethane solvent. The extraction was allowed to proceed for 8 hrs until the aldrin was washed off the polymer.

## 4.5 Development of films

The prepared MI-PANI nanoparticles were deposited on glass substrates. Before deposition, the glass substrates were washed with acetone, then methanol and finally distilled water. After which they were placed in an oven and dried at 60 $^{o}$C.

The method used for deposition was the dip coating method. In this method, the pre cleaned glass substrate was dipped for 5 min into the polyaniline nanoparticles dispersed in chloroform, and then withdrawn from the solution slowly to ensure the fluid had time to flow back down into the solution. The glass substrate was then held horizontally with the applied coating and left for 10 min until the solvent evaporated to leave a thin film.

## 4.6 Electrical measurements

Three pellets were pressed from the same batch of neat PANI powder i.e. 200 mg, 300 mg, 400mg with thicknesses 1.27 mm 1.89 mm and 2.96 mm respectively. Pellets with a diameter of 13.05 mm were prepared so as to compare their conductivities. Pellets were prepared from the aldrin MIP powder with a thickness and diameter of 1.27 mm and 13.05 mm respectively. All pellets were pressed at a hydraulic pressure of 10 MPa and used in determination of the conductivity of MIP. The four-probe method (pressure contact) was used to measure the conductivity. A Solartron-Schlumberger 7841 digital multimeter, a Keithley 220 current source, and a Keithley 705 scanner with a Keithley 7052 matrix scanner card were used in the experimental setup. The measurements were carried out at room temperature.

## 4.7 Rebinding Experiments

The binding capacity of the imprinted nanoparticles was determined using 40 mg of MI-PANI added into 5 test tubes with 1 ml of aldrin at concentrations ranging from 1 ng/µL to 5 ng/µL in hexane at room temperature for 20 hours with shaking. The polymer particles were then allowed to settle for 30 min. The concentration of free aldrin in the solution was assayed by Gas Chromatography-Time of Flight Mass Spectrometry (GC-TOFMS). The amount of bound analyte (B) to the molecularly imprinted polyaniline (MI-PANI) was calculated by subtracting the amount of free analyte (F) from the initial concentration. The selectivity of the MI PANI was investigated by comparing the adsorption of aldrin and DDT on the MIP. All data obtained in the experiments were processed by OriginPro 8.1 software.

# CHAPTER 5

# RESULTS AND DISCUSSION

## 5.1 Introduction

This chapter discusses the results from the characterisation experiments carried out during the course of the study. These include techniques for structural analysis such as Fourier Transform Infrared (FTIR), Proton Nuclear Magnetic Resonance ($^1$H-NMR), Ultra-Violet visible (UV-VIS) and those for morphology characterisation such as Scanning Electron Microscopy (SEM), Atomic Force Microscopy (AFM) and X-ray diffraction (XRD). The electrical properties were evaluated using four point probe coupled to source meter. The results from the adsorption studies are also discussed.

## 5.2 Structural Characterisation

## 5.2.1 Fourier Transform Infra Red (FTIR)

Fourier Transform Infrared (FTIR) spectroscopy is a widely used technique for characterising materials. The spectrum produced from the analysis gives the identity of that particular sample. The absorption peak frequencies correspond to characteristic vibrations of bonds between atoms that make up the material. Thus, the FTIR spectrum is characteristic of a material and provides positive identification.

### 5.2.1.1 FTIR Spectral Studies on Polyaniline

In order to confirm that polyaniline was synthesised, FTIR spectroscopic analysis was conducted to evaluate functional groups in the synthesised polyaniline. Figure 14 shows the FTIR spectrum of PANI nanoparticles prepared at room temperature. In the FTIR spectrum, the peak at 796 $cm^{-1}$ is attributed to out of plane bending vibration of C-H on para-disubstituted rings which is consistent with the proposed tetra substituted benzene ring system [55]. Moreover, it is also supported by the earlier reports that benzene ring is connected at para position with quinonediimine

moieties and the out of plane bending vibration lies at 830 $cm^{-1}$ [56]. The bands at 1570 $cm^{-1}$ are due to the stretching vibration of C=C quinoid ring. Characteristic peak at 1480 $cm^{-1}$ [56] is due to the stretching vibration of C=C of benzenoid ring while the bands at the 1294 $cm^{-1}$ and 1236 $cm^{-1}$ are ascribed to the C-N stretching mode of the aromatic amine. The strongest peak at 1120 $cm^{-1}$ is assigned to the vibration mode of $–NH^{+}=$, indicating a higher doping level [57]. Normally, a polymer that exhibits charge delocalization shows absorption at around 1140 $cm^{-1}$. The charge delocalisation band for polyaniline HCl were reported at 1125 $cm^{-1}$[58, 59]. The absorption band at 3450 $cm^{-1}$ is due to the N-H stretching mode. In general, anilinium ion displays a strong and broad band in the region 3400 $cm^{-1}$ – 3030 $cm^{-1}$ due to N-H stretching vibration whereas N-H bending vibration appears at around 1302 $cm^{-1}$ – 1289 $cm^{-1}$ [60]. All the observed characteristic IR absorption bands for polyaniline are summarized in Table 3. Therefore, the FTIR spectroscopic analysis supported the observation that the prepared polymer nanoparticles consisted of polyaniline.

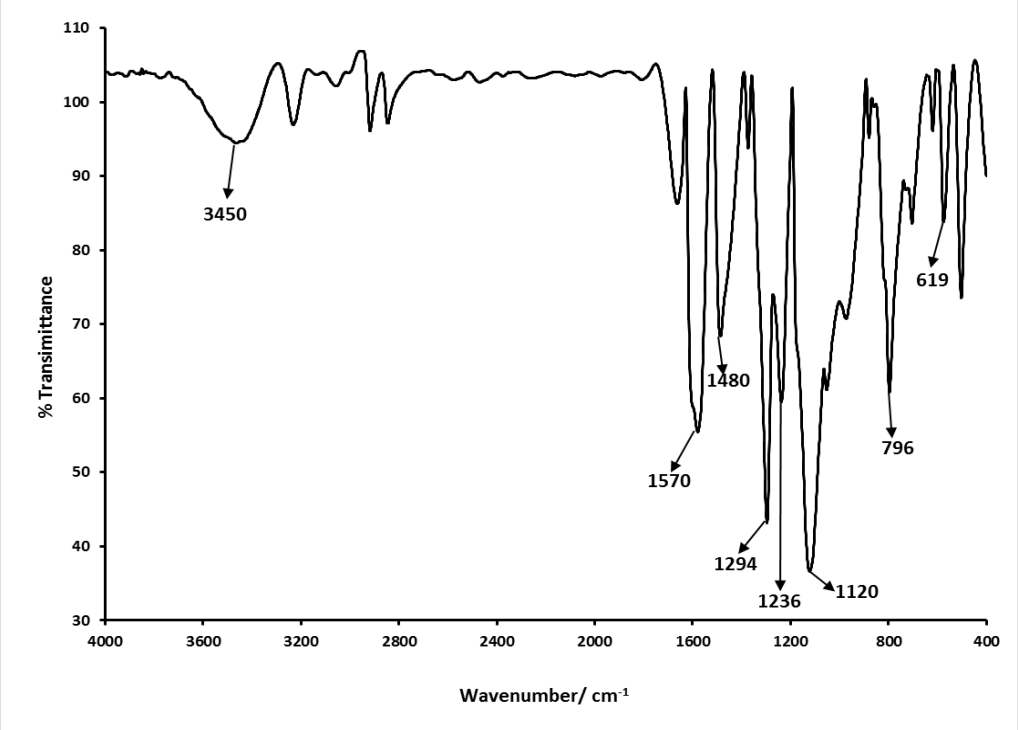


**Figure 14: FTIR spectrum of neat polyaniline nanoparticles.**

**Table 3: FTIR observed peaks and expected vibrations for polyaniline nanoparticles.**

| Observed peaks position ($cm^{-1}$) | Expected vibrations |
|---|---|
| 3450 | N-H stretching vibration |
| 1570 | C=C quinoid ring |
| 1480 | C=C of benzenoid ring |
| 1294<br>1236 | C-N stretching mode of the aromatic amine |
| 1120 | $–NH^{+}=$ vibration mode |
| 796 | C-H out of plane bending vibration |
| 619 | Aromatic ring |

## 5.2.1.2 FTIR spectral studies on Aldrin MI-PANI

FTIR characterisation was performed to determine the functional groups in MI-PANI before and after the template extraction (washing) by using the KBr pellet method. It can be observed from Figure 15 below that the absorbance peaks for all spectra (MIP before and after the washing stage and neat PANI) are identical except for the intensity. Furthermore, the absorbance peak of N-H band at 3450 $cm^{-1}$ is missing in spectra b (see Figure 15) due to the fact that interaction occurred between the template (aldrin) and the polymer. This confirmed that there was effective imprinting. The rest of the peaks at 1579 $cm^{-1}$, 1484 $cm^{-1}$, 1117 $cm^{-1}$, 794 $cm^{-1}$ are all in the polyaniline backbone and they are elaborately explained in section 5.2.1.1 above.

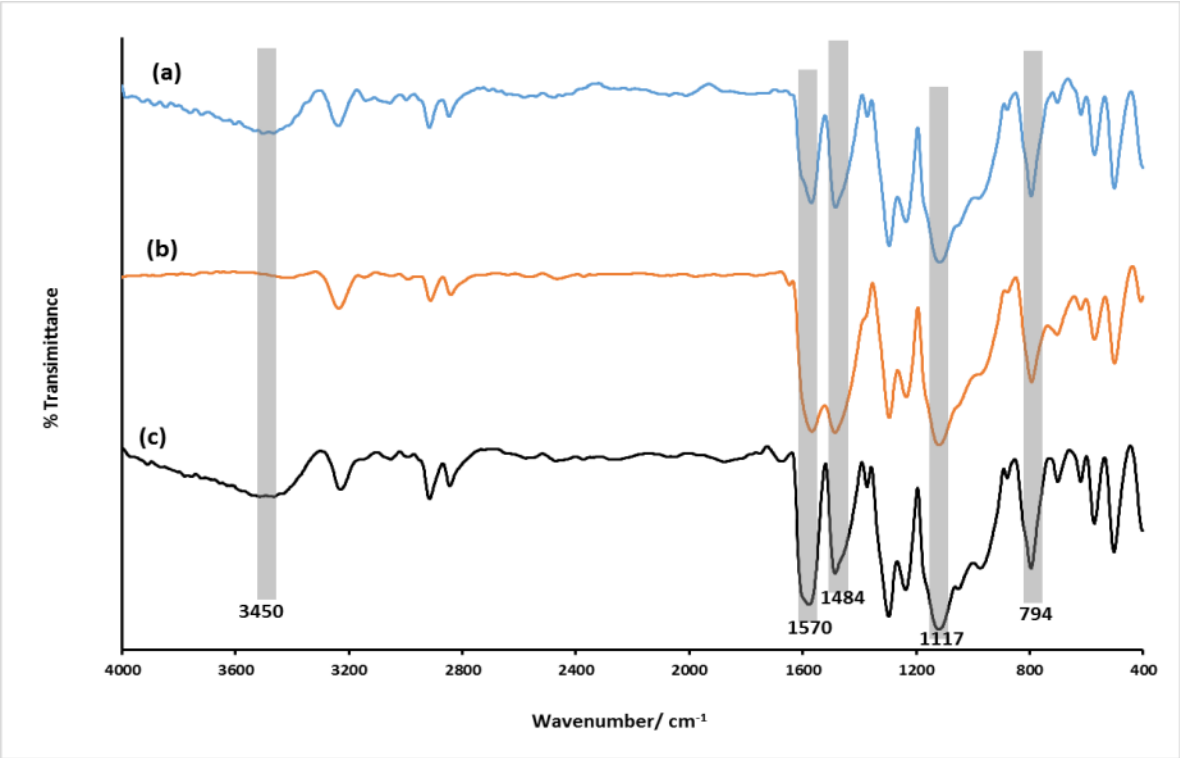


**Figure 15 : FTIR spectra of Aldrin MI-PANI (a) after extraction, (b) before extraction (c) NIP**

## 5.2.2 $^{1}$H- NMR Spectra

### 5.2.2.1 $^{1}$H- NMR Spectra of neat Polyaniline

Typical $^{1}$H- NMR spectra of neat PANI prepared at room temperature are shown in Figure 16. From the spectra, it can be observed that the PANI polymer exhibit the strongest sharp peak in the region 7 ppm to 7.68 ppm which are due to aromatic protons of the quinoid and benzenoid ring. The resonance at δ 3.66 ppm in the spectra of the polyaniline salt is assigned to the N –H groups. The peaks at δ 1.35 ppm and 8.12 ppm, 8.13 ppm may be due to the water protons bonded by (-$NH_2$) groups and (H-$N^+$).

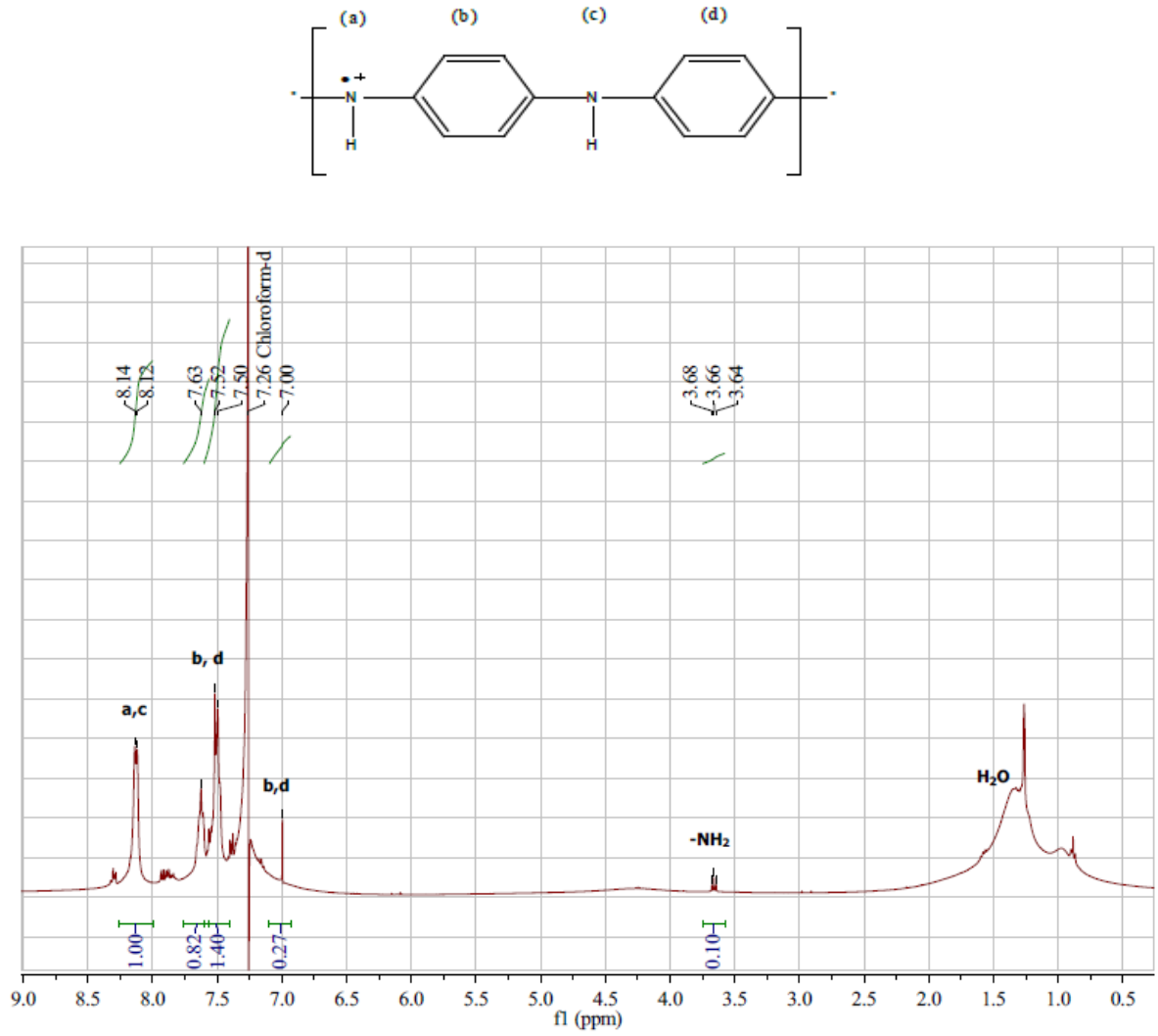


**Figure 16: $^{1}$H-NMR spectrum of the synthesized polymer polyaniline salt obtained by emulsion polymerisation.**

## 5.2.2.2 $^{1}$H- NMR Spectra of Aldrin MI-PANI

Figure 17 shows $^{1}$H-NMR spectrum of Aldrin MI-PANI. With reference to aldrin structure given below, it is reported that the $^{1}$H-NMR spectra of aldrin [61] indicates that resonance due to protons 1 and 2 which occur at δ 6 ppm and is in the form of a mulitiplet. Similarly, the peaks due to 7 and 8 protons are multiplets because of spin – spin splitting and are centred at 2.7 ppm .The δ 2.2 ppm signals are assigned to protons 3 and 4. Finally the methylene protons 5 and 6 which are anti-bridge and syn-bridge to other give peaks at δ 1.5 ppm. It can be observed form Figure 17, all

the peaks attributed to the aromatic protons of the benzenoid and quinoid ring are present in the region 7 ppm to 7.64 ppm reported in Figure 16 above. However, additional peaks arising from proton in the aldrin structure are observed at δ 1.56 ppm, 1.58 ppm, 1.60 ppm which can be attributed to the methylene protons in aldrin. The peaks at δ 2.7 ppm and 2.9 ppm can be attributed to proton 3 and 4 in the aldrin structure shown below. The peak at 5.17 ppm is due to the presence of proton 1 and 2 though we note that there are shifts in position due to chemical interactions which may have taken place during the reaction. Figure 17 shows the appearance of a peak at around 5.17 ppm and 1,56 ppm, 1.58 ppm, 1.6 ppm in the spectrum of the aldrin MIP , assigned to the protons in aldrin moiety , which is absent on the spectrum of the neat PANI. This was taken as clear evidence that the modification was successful. The observed peak positions in the aldrin – MIP are tabulated in Table 4.

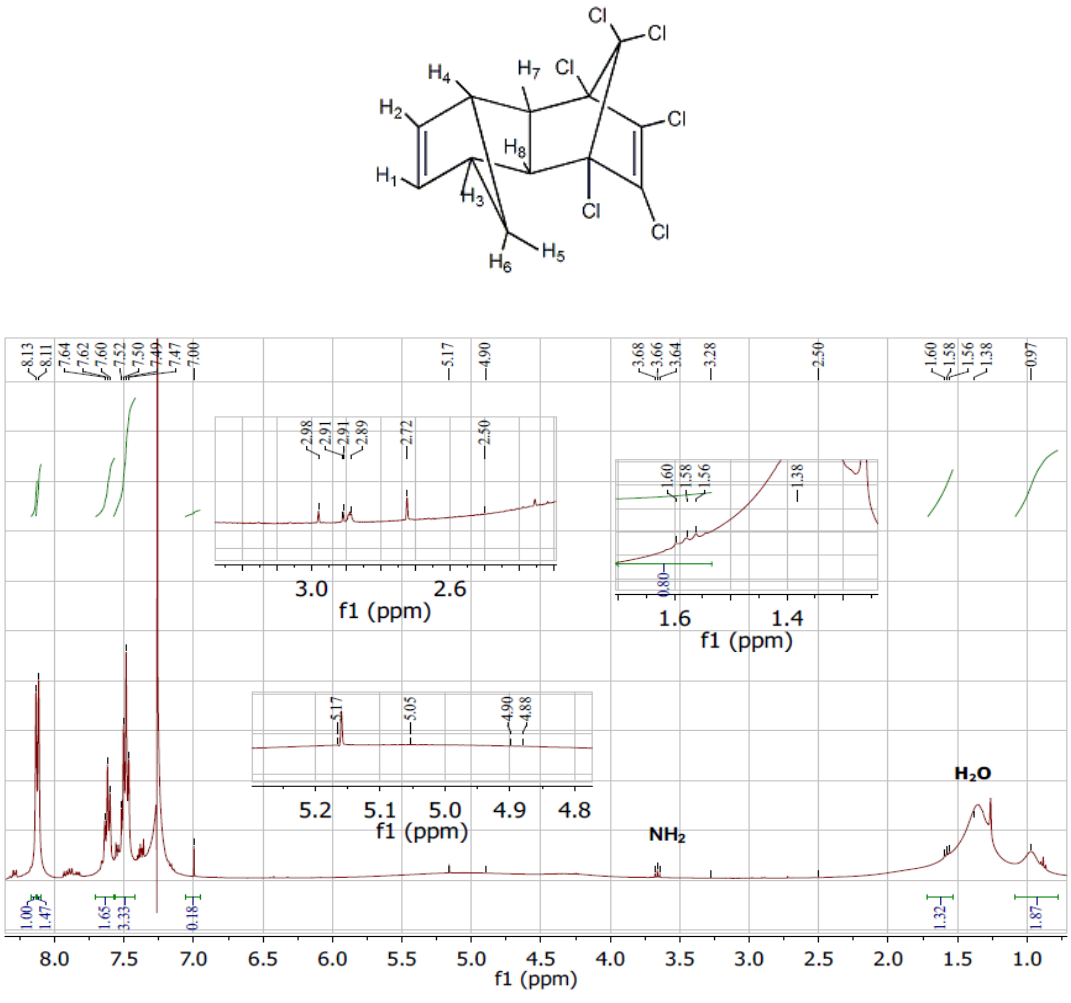


**Figure 17: $^{1}$H-NMR spectra of the synthesized Aldrin MI-PANI.**

**Table 4: H-NMR chemicals shift position of Aldrin and Aldrin MI-PANI.**

| **Compound** | | **Chemical** | **Shift δ** | **(ppm)** | |
|---|---|---|---|---|---|
| | **1,2** | **3,4** | **5** | **6** | **7,8** |
| Aldrin | 6.18 | 2.26 | 1.56 | 1.06 | 2.72 |
| Aldrin MI-PANI | 5.17 | 2.35 | 1.56,1.58, 1.6 | 0.97 | 2.72 |

## 5.2.3 UV-Visible studies

UV-VIS studies were further carried out to validate the structure of polyaniline. The UV-VIS spectra of PANI doped with HCl is shown in Figure 18. It can be observed that the spectrum has three major absorption peaks. The peak at 360 nm is attributed to $\pi \rightarrow \pi^*$ transition of the benzenoid rings, an indication of the transition of electron from the highest occupied molecular orbital (HOMO) to the lowest unoccupied molecular orbital (LUMO). The peaks at 430 nm and 825 nm can be assigned to polaron transition [62, 63] , indicating that the samples are conductive emeraldine salt (ES) form. These are also in good agreement with the earlier reports that these polarons are the dominant species in the conductance process [62, 63].

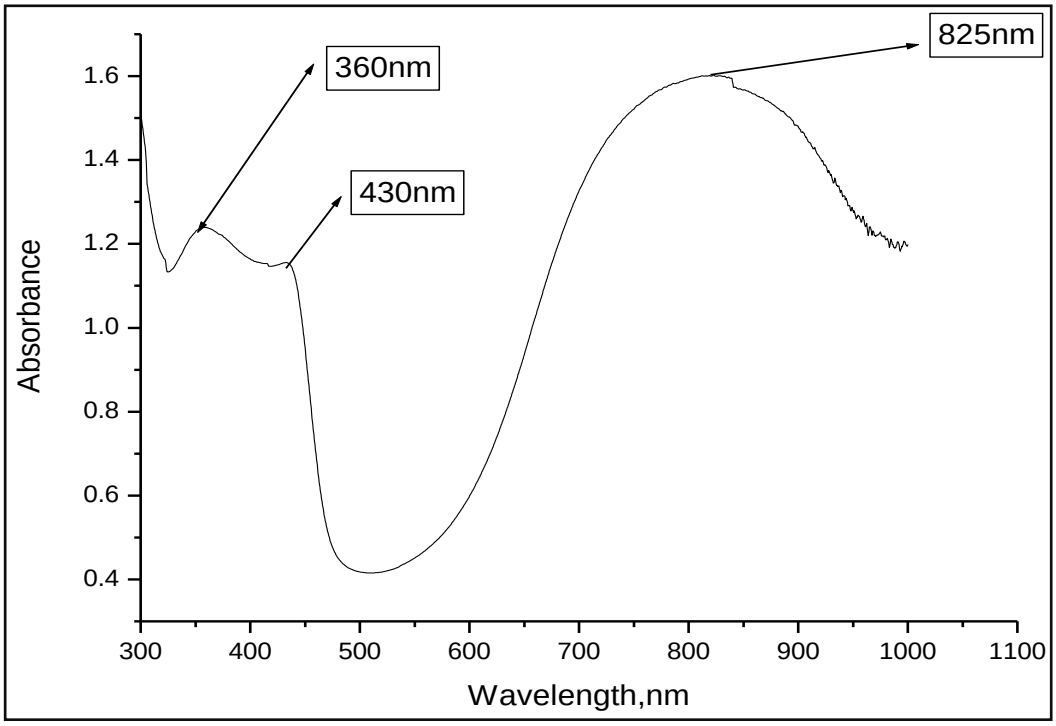


**Figure 18: UV-Vis spectrum of the synthesized polyaniline nanoparticles.**

## 5.3 Morphological Analysis

## 5.3.1 SEM Analysis

### 5.3.1.1 SEM Analysis of Neat Polyaniline nanopartcles.

Scanning electron microscopy studies were carried out to evaluate the shape and size of the synthesized polyaniline nanoparticles. Figure 19 shows the SEM images taken from the thin films of the non imprinted polyaniline nanoparticles. SEM images were done with 1 kV electron beam energy. The scanning electron micrographs shown in Figure 19 revealed that the prepared nanoparticles have a perfect spherical shape with particle size ranging from 60 nm-100 nm. The surface of the non imprinted polyaniline was generally smooth.

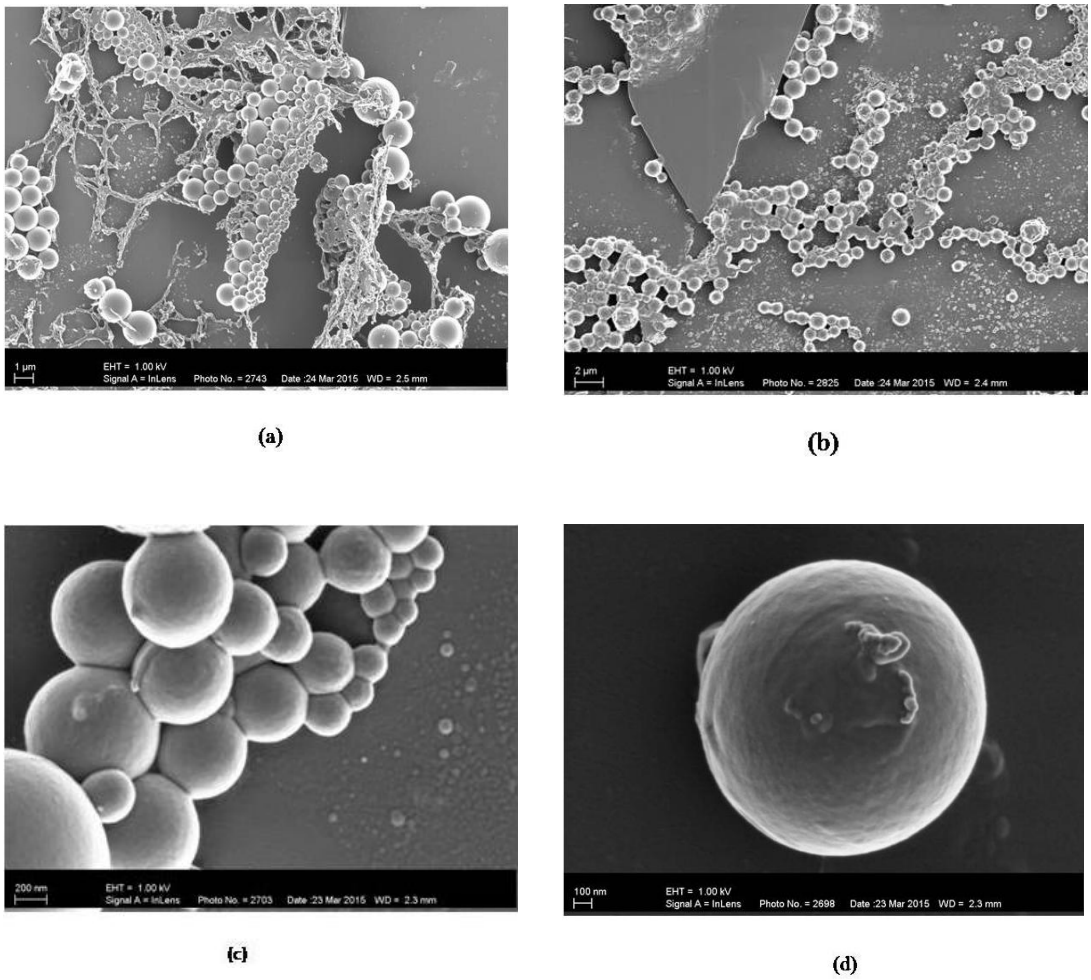


**Figure 19: Scanning electron micrographs of non imprinted polyaniline (1.00kV beam energy).**

## 5.3.1.2 SEM analysis of Aldrin MI PANI

Typical SEM micrographs for molecularly imprinted polyaniline thin films are shown in Figure 20. The images were taken at different locations of the films so as to have a clear indication of the morphology of the films. From the images, it can be observed that the MIP particles are spherical in shape with size ranging from 500 nm to 1.8 μm. It is evident that the size of the MIP particles increased greatly as compared to the non imprinted polymers (as seen in Figures 19(a) and 20(a)). Also the surface is rough as compared to the smooth surface observed in neat polyaniline nanoparticles. The other observation made is that particles position themselves in clusters and on specific portions of the film. The clustering of the particles could have been due to agglomeration of the primary particles which could be attributed to either van der waals forces.

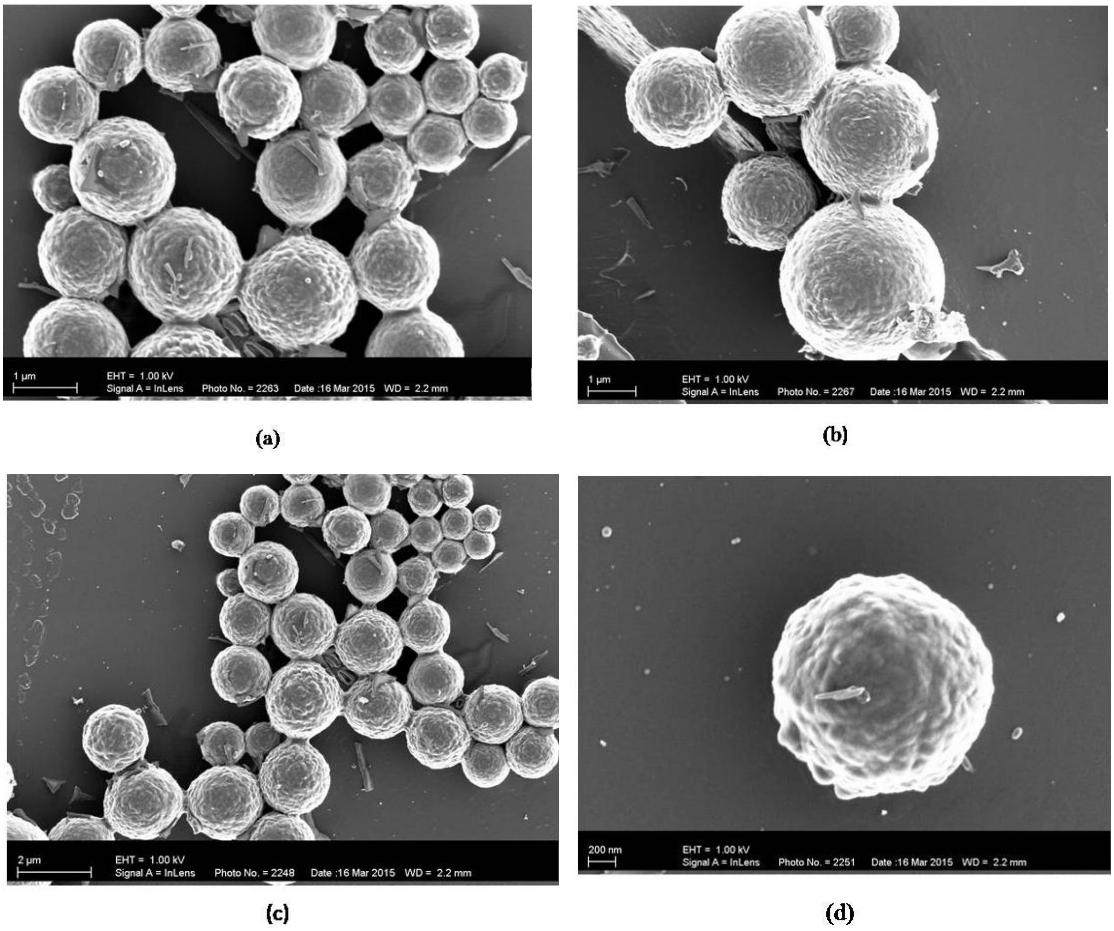


**Figure 20: Scanning electron micrographs of Aldrin Molecularly Imprinted Polymers (1.00KV beam energy).**

## 5.3.2 Atomic Force Microscopy Studies

### 5.3.2.1 AFM Studies of Neat polyaniline Nanoparticles

Atomic Force Microscopy studies were carried out to further evaluate the morphology of the neat polyaniline and MI-PANI nanoparticles. Figure 21 shows 5μm scanned AFM 3D height images for the PANI thin films done in contact mode. It is clear from the AFM image that the film consists of a thin layer of small spherical nanoparticles with an average size of 65 nm which corroborates the SEM results in section 5.3.1.1. The AFM images further confirm that the nanoparticles are successfully synthesized according to plan.

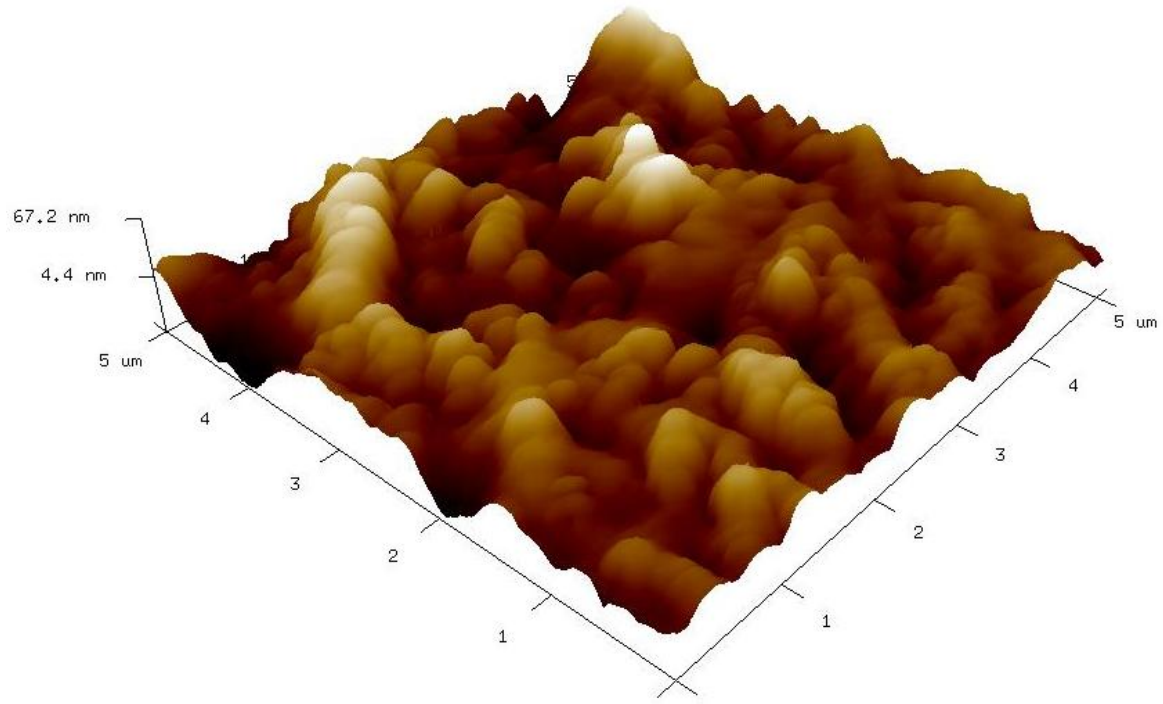


**Figure 21: AFM micrographs of the synthesised polyaniline nanoparticles**

## 5.3.2.2 AFM Studies of MI-PANI

AFM studies were also carried out on molecularly imprinted polyaniline in order to study the surface morphology of the imprinted films. Figure 22 shows the 5μm scanned AFM 3D height image for the MI-PANI thin films done in contact mode. The result showed that the particles were spherical in shape with a general increase in particle size to an average of 600 nm. The increase in size is attributed to incorporation of template during polymerisation process. The roughness average value for the non imprinted PANI was found to be 53 nm while that of the imprinted PANI was 0.017 μm as determined from Gwyddion software. This result corroborates the SEM results obtained in section 5.3.1.2.

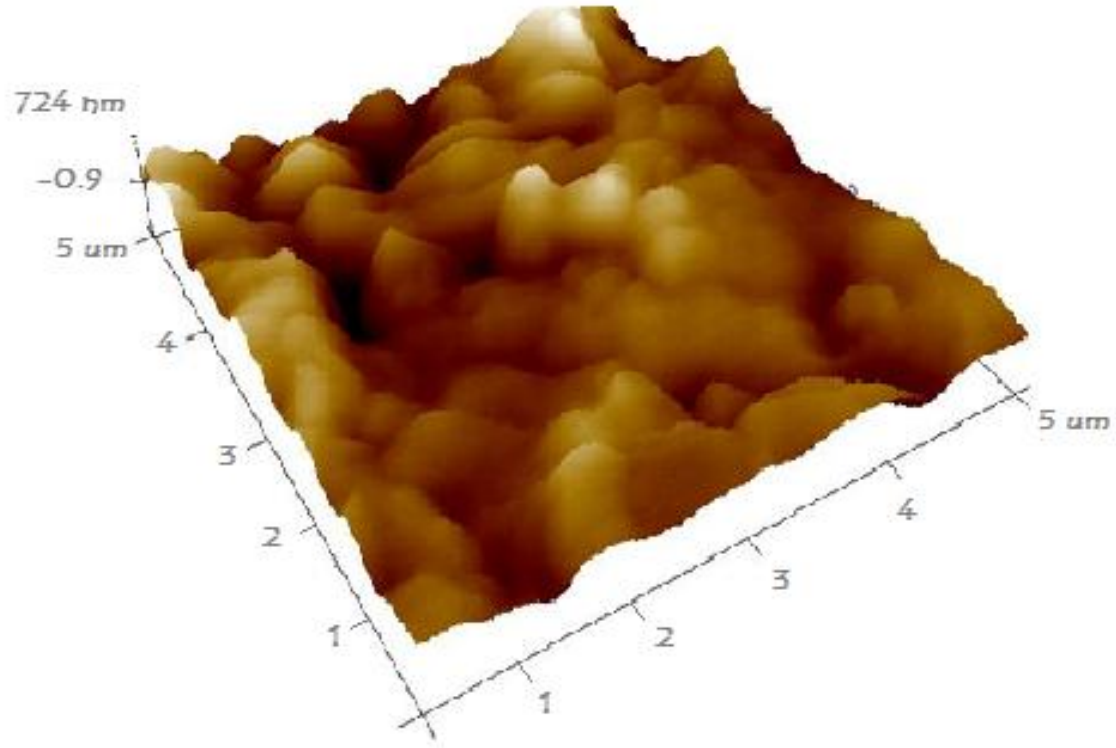


**Figure 22: AFM micrographs of the synthesised molecularly imprinted polyaniline nanoparticles.**

## 5.3.3 XRD Spectra

The behaviour of solids stems from the arrangement and properties of constituent atoms. The arrangement leads to bulk properties that include rigidity, brittleness and electrical conductivity. Since the wavelength of X-rays is comparable to the size of atoms, they are ideally suited for probing the structural arrangement of atoms and molecules in a wide range of materials. Energetic X-rays can penetrate deep into the materials and provide information about the bulk structure. Information from XRD measurements provides "finger prints" of materials that can be used for identification or verification of the integrity of the materials. This is because the distribution of diffraction angles, and therefore peak position and intensities for each material is unique.

## 5.3.3.1 XRD Spectra for Polyaniline

The crystallinity of the synthesized polyaniline nanoparticles was assessed from powder X-ray diffraction (XRD) patterns. The results of the XRD analysis of the synthesized polyaniline nanoparticles are shown in Figure 23 and tabulated in Table 5. All the PANI three peaks are observed at $17.52^{o}$, $23.3^{o}$, $29.41^{o}$ and $31.63^{o}$ 2θ, with d-spacing 6.33 Å, 4.59 Å, 4.33 Å and 3.28 Å respectively. The shifting in position of the peaks in the XRD spectra obtained from the typical PANI XRD spectra is due to the fact that these XRD results were obtained with a Co-Kα radiation as compared to the commonly used Cu- Kα radiation. However, the XRD pattern of PANI nanoparticles synthesized exhibited sharp peaks at $2\theta = 23.3^{o}$ and $29.41^{o}$ indicating the presence of high crystallinity and condensed structure. The peak centered at $2\theta = 23.3^{o}$ is ascribed to periodicity parallel to the polymer chain and the latter peak maybe caused by the periodicity to the polymer chain [64]. This crystalline structure could be explained by the fact that the PANI nanospheres were prepared in nanosize micelles, thus proceeded in denser and more compact structures. These results are in good agreement with the relationship between the

crystallinity of conducting polymer and its electrical conductivity: the greater the degree of crystallinity, the higher the conductivity [65].

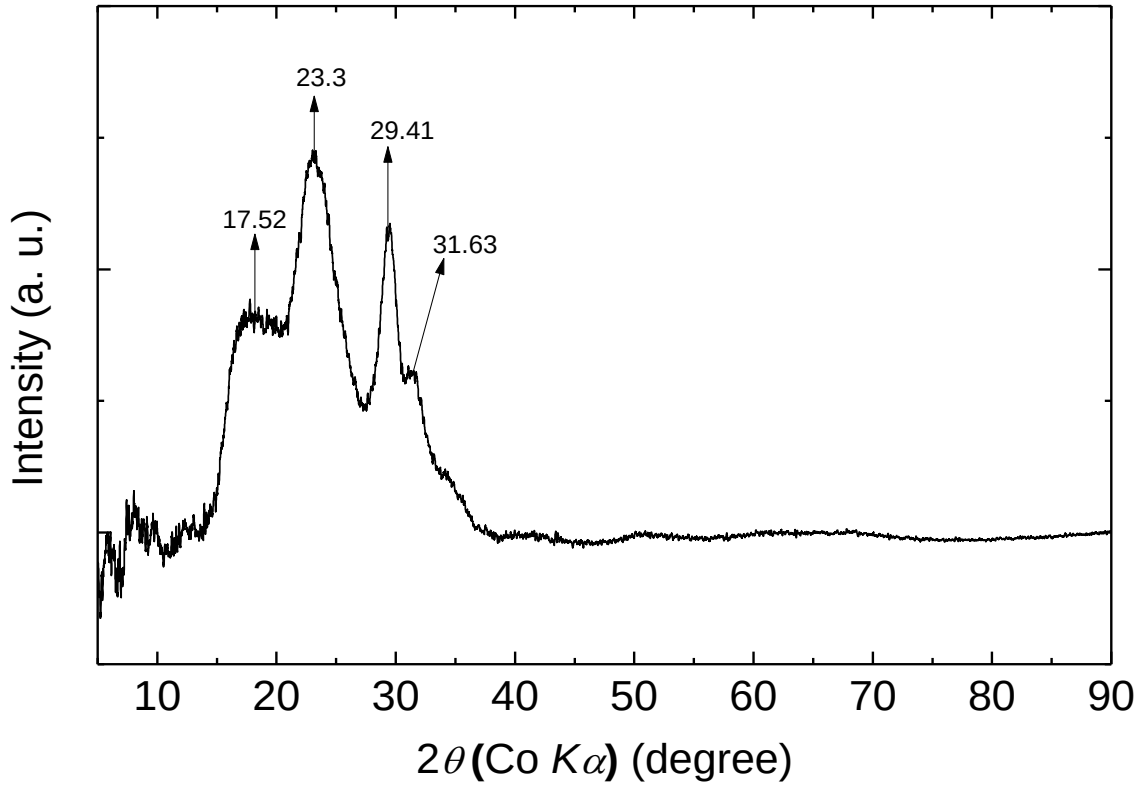


**Figure 23: XRD spectra of polyaniline nanoparticles synthesized at room temperature.**

**Table 5: Polyaniline XRD peak positions and d-spacing.**

| Peak No. | Position [ $^{o}2\theta$] | d-spacing [Å] |
|---|---|---|
| **1** | 17.52 | 6.33 |
| **2** | 23.30 | 4.59 |
| **3** | 29.41 | 4.33 |
| **4** | 31.63 | 3.28 |

## 5.4 Electrical characterisation

The primary means of electrical characterisation for all the polymers prepared was through current – voltage measurements. This was accomplished through use of the 4-probe technique. The four-point probe consists of four conductive metal probes that are in line. Current is injected and collected through the two outer probes, while the potential drop between the two inner probes is monitored. The current- voltage measurements were carried out at a start current and end current of 10 μA and 50 μA respectively. By use of four point probe labview analysis software, the voltage /current curves as well as resistivity/current curves were obtained and are shown in Figures 24 and 25.

Figures 24 and 25 illustrate room temperature voltage-current characteristics of PANI and aldrin MI-PANI pellet. These figures indicate that the conductivity of PANI and of MI-PANI obey ohmic behaviour at room temperature.

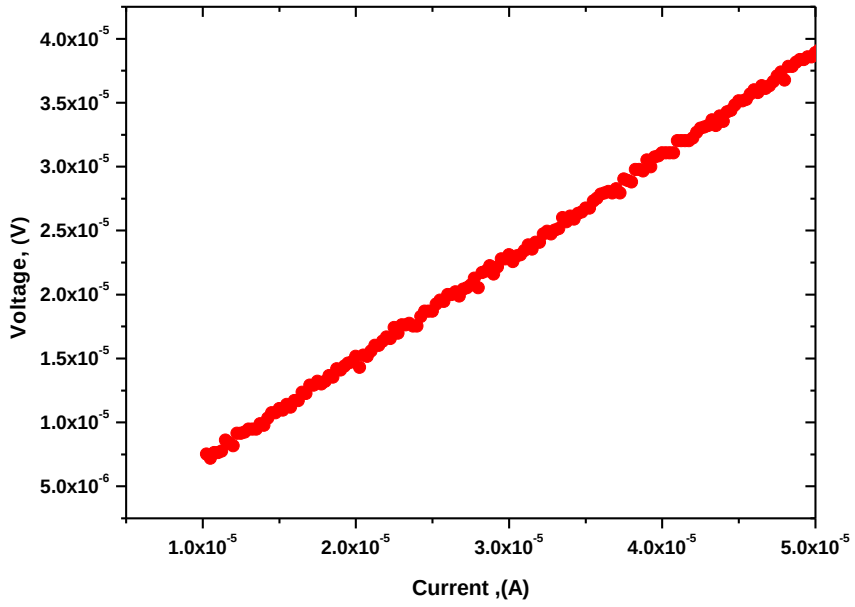


**Figure 24: Room temperature current-voltage characteristics for PANI pellet pressed at 10MPa.**

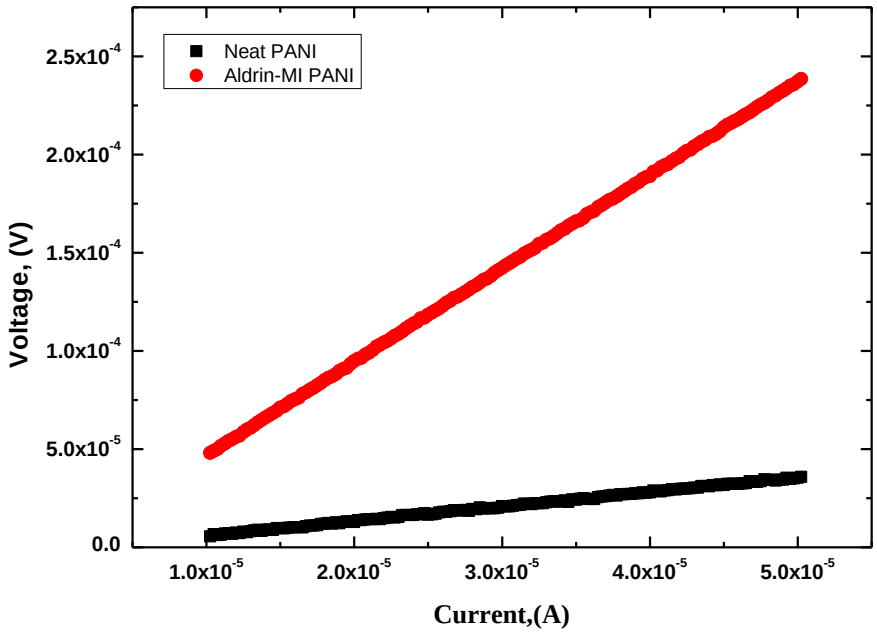


**Figure 25: Room temperature current-voltage characteristics for PANI and Aldrin MI-PANI pressed at 10MPa.**

From resistivity–current curves, it was observed that the resistivity of polyaniline drastically increased after imprinting with aldrin as can be shown in Figure 26. In CPs, electronic charge transport requires motion of charge along the polymer backbone. It has been demonstrated that in order to allow the formation of delocalized electronic states, CPs molecular arrangement must be conjugated [12]. The delocalization of the electronic states relies on the resonance stabilized structure of the polymer. The decrease in conductivity of polyaniline after imprinting with aldrin can be attributed to disturbance of the charge transport along the polymer chain as the template is embedded in the polymer matrix.

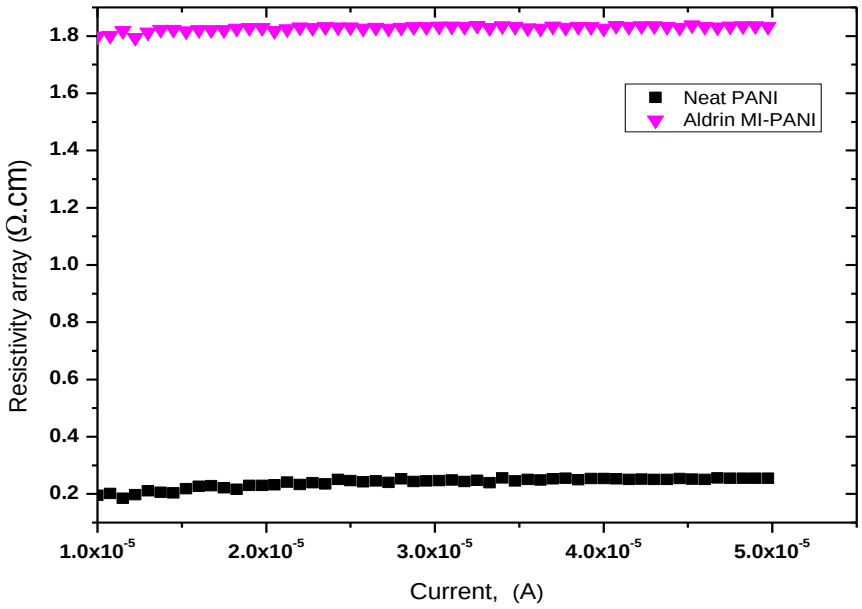


**Figure 26: Resistivity-Current characteristics for three PANI pellets and Aldrin MI-PANI pressed at 10MPa.**

## 5.5 Rebinding Experiments

In order to evaluate the binding capacity of the imprinted polymer, it is important to make an estimation of the binding properties of the system. The binding properties of the imprinted polymer are evaluated through adsorption isotherms. An adsorption isotherm is a measure of the relationship between the concentration of bound and free guest in a given system. Thus, the obtained Molecularly Imprinted Polymer (MIP) was evaluated by rebinding experiments and the experimental adsorption isotherms fitted into the mathematical models the Langmuir isotherm.

## 5.6 Equilibrium rebinding analysis

In order to investigate the aldrin binding characteristics on the imprinted polymers, the binding isotherm was determined in the range of 1.4 - 5.0 ng/μg as the initial concentrations of aldrin. The bound aldrin concentration as well as the free aldrin in hexane is given in Table 6. These concentration values are obtained by the procedure described in section 4.7.

**Table 6: Concentration of Aldrin in the sample solutions.**

| Sample | Initial Aldrin concentration (ng/μL) | Aldrin concentration at equilibrium ($C_e$) ng/μL | Bound Aldrin (ng/μL) |
|---|---|---|---|
| **M1** | 5 | 4.1 | 0.9 |
| **M2** | 4 | 3.4 | 0.6 |
| **M3** | 3 | 2.5 | 0.5 |
| **M4** | 2 | 1.8 | 0.2 |
| **M5** | 1.4 | 1.3 | 0.1 |

Figure 27 shows the binding profile of aldrin onto the MI-PANI. The plot was obtained by plotting the saturated adsorbed amounts of aldrin against initial concentrations of the aldrin in hexane solution. In the studied concentration range, the aldrin adsorption amount increases with the increasing amount of the aldrin

initial concentration. This indicates that there are specific rebinding sites on the imprinted polymers.

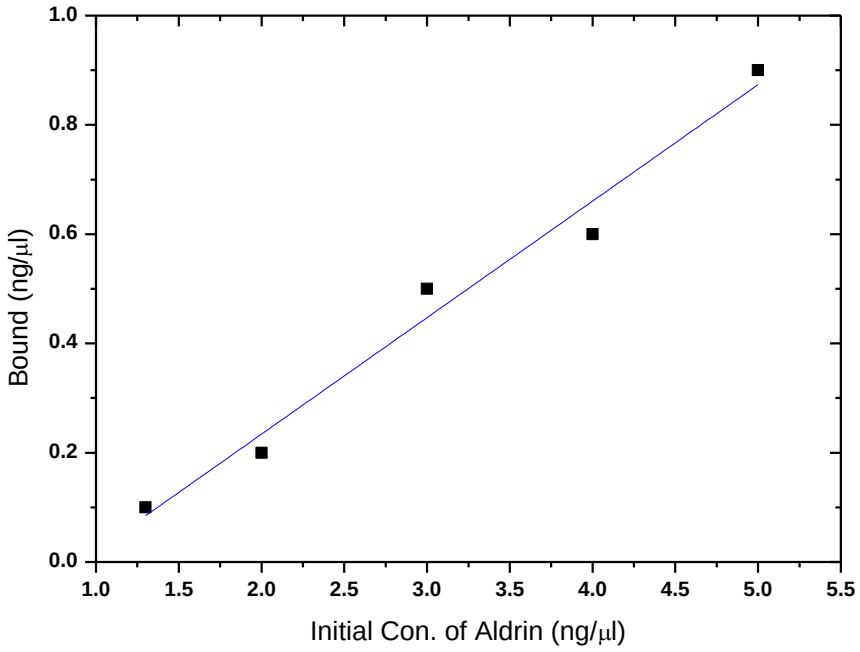


**Figure 27: Binding profile of aldrin onto PANI nanoparticles.**

The data obtained in the batch binding experiment were fitted by Langmuir model (shown in Figure 28). Langmuir adsorption isotherm is one of the most famous and widely-used adsorption isotherm. The Langmuir equation is as shown below:

$$B = \frac{B_{max} \times C}{K_D + C}$$

Where $K_D$ is the equilibrium dissociation constant, C is the free equilibrium concentration of aldrin, and $B_{max}$ is the apparent maximum number of aldrin molecules binding on the polymers. From Figure 28 it can be observed that at equilibrium concentration higher than 3.58 ng/μ, adsorption of MIPs became stable as its recognition sites were almost saturated. Therefore, the apparent maximum amount of bound aldrin ($B_{max}$) and the point of saturation are established to be 0.799 ng/μL and 3.58 ng/μL respectively.

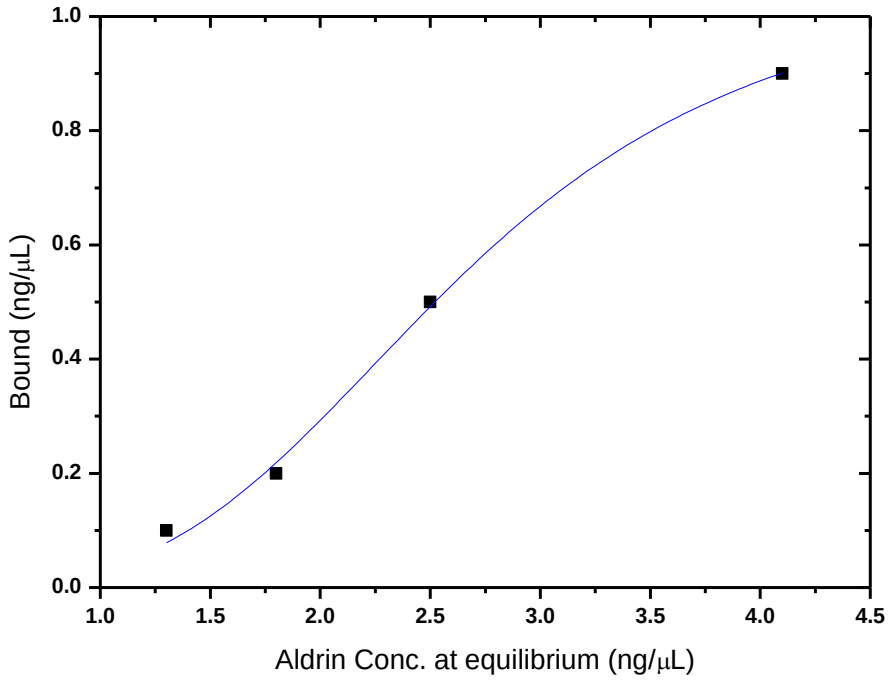


**Figure 28: Langmuir adsorption isotherm results of MI-PANI.**

Scatchard analysis was employed to further analyse the binding isotherms, which is an approximate model commonly used to estimate the binding parameters of MIPs. The scatchard equation can be expressed as follows:

$$\frac{B}{C} = \frac{B_{max} - B}{K_D}$$

where $K_D$ is defined as the equilibrium dissociation constant of the binding sites, B is the amount of aldrin bound to the polymer, $B_{max}$ is the maximum adsorption amounts of aldrin on the polymer, and C is the equilibrium concentration of aldrin in the solution. Figure 29 shows the scatchard plot of the binding of aldrin to the MI- PANI.

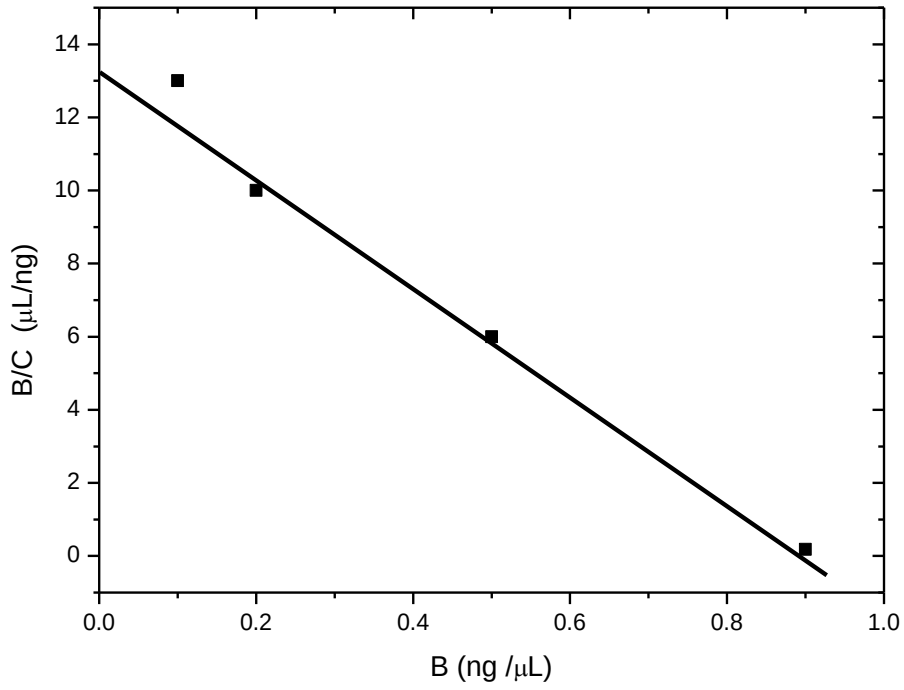


**Figure 29: Scatchard plots of the synthesized Molecularly Imprinted Polyaniline nanopartcles.**

It is clear that the scatchard plot for MI-PANI is a single straight line. The linear regression equation was, B/C= -15.32x + 13.28 ($R^2$ =0.987), suggesting that the homogeneous recognition sites for aldrin were formed in the MI-PANI. From the slope, -15.32 = $1/K_D$, where $K_D$ is the equilibrium dissociation constant of the binding sites. From the intercept, 13.28 = $B_{max}/K_D$, where $B_{max}$ is the maximum adsorption amounts of aldrin on the polymer. $K_D$ and $B_{max}$ were calculated to be 0.06 ng/μL and 0.799 ng/μL respectively.

## 5.7 Molecular selectivity of MI-PANI

In order to verify that imprinted polymers are selective to aldrin, the binding of aldrin and a structurally related compound was investigated. DDT was chosen as the reference for investigating the specific selectivity. Its structure is shown in Figure 1 Section 1.1. The imprinted polymers exhibited high binding affinity for aldrin, while the structurally related compound DDT used showed less binding capacity.

The distribution coefficient $K_D$ was utilised to evaluate the molecular selectivity of MI- PANI. $K_D$ is defined as follows:

$$K_D=C_p/C_s$$

where $C_p$ (ng/μL) is the amount of adsorbed aldrin on MI-PANI and $C_s$ (ng/μL) is the equilibrium concentration of substrates in solution. Table 7 shows the K values of the two tested compounds.

**Table 7: Comparison of distribution coefficient of Aldrin and DDT.**

| Substrate | Initial concentration (ng/μL) | Concentration at equilibrium ng/μL | Bound (ng/μL) | Distribution coefficient K (μL/ng) |
|---|---|---|---|---|
| **Aldrin** | 3 | 1.3 | 1.7 | 1.31 |
| **DDT** | 3 | 1.7 | 1.3 | 0.76 |

A linear function is the simplest and most widely used adsorption isotherm equation which is conventionally expressed in terms of the distribution coefficient $K_D$. It can be seen that MI- PANI exhibited a high distribution coefficient (1.31) for aldrin than that of DDT (0.76). The high $K_D$ value obtained for aldrin suggests the presence of certain cross-binding reactivity which is evidence that the imprinting method created cavities based on the shape selection and position of functional groups that recognised template (aldrin). Therefore, MI- PANI exhibit much stronger affinity for aldrin than for DDT, hence is selective towards aldrin.

# CHAPTER 6

# CONCLUSIONS

## 6.1 Introduction

This chapter contains the overall conclusions of the results obtained in this study as well as possible future work.

## 6.2 Overall Conclusion

The present work has demonstrated that molecular imprinting technology can be employed to produce a molecularly imprinted conducting polymer using aniline as a functional monomer and aldrin as analyte of interest. The synthesized MI-PANI was identified by FTIR and $^{1}$H-NMR**.** From SEM analysis, the particles obtained were spherical with MI-PANI NPs diameters ranging from 500 nm – 1.8 μm. PANI NPs diameters were in the range of 60 nm-100 nm. MI-PANI exhibited electrical conductivity of 0.546 S/cm while neat PANI had a conductivity of 4.149 S/cm. From binding kinetics: Langmuir adsorption isotherm and scatchard analysis, the apparent maximum amount of bound aldrin and the point of saturation is 0.799 ng/μL and 3.58 ng/μL respectively. The specificity and selectivity of the imprinted polymers were investigated by binding analysis using aldrin and DDT. The results indicated that the imprinted polymers showed a good selectivity and specificity for aldrin. Therefore, the synthesized polymers can be used as active layers, for selective and sensitive detection of aldrin in chemical sensors.

## 6.3 Future Work

The work described in the preceding chapters is only one step in the direction to optimize and design of operative chemical sensor based on molecularly imprinted polyaniline. Future work should put attention to effective extraction of aldrin from the imprinted sites so that the sensing characteristics of the sensor are improved.

Furthermore, future work should pay attention to evaluation of possible application of the molecularly imprinted polyaniline in solid phase extraction (SPE) of pollutants, especially pesticides from the environment.

# REFERENCES


1. Ritter, L and J. Forget, 1995. "Persistent Organic Pollutant. " , An Assessment Report on: DDT-Aldrin-Dieldrin-Endrin-Chlordane- Heptachlor-Hexachlorobenzene- Mirex-Toxaphene Polychlorinated Biphenyls Dioxins and Furans.
2. Alexander, C., H. S. Andersson., L. I. Ansell., R. J. Kirsch., N. Nicholls., I. O'mahony and M. J. Whitcombe., 2006. "Molecular imprinting science and technology: a survey of the literature for the years up to and including 2003." J. Mol. Recognit.,19,106–180.
3. Lange, U., N.V. Roznyatovskaya and V.M. Mirsky. 2008. "Conducting Polymers in Chemical Sensors and arrays." Analytica chimica acta. 614(1), 1-26.
4. Shirakwa, H.,1977. "Synthesis of electrically conducting organic polymers: halogen derivatives of polyacetylene, $(CH)_x$." Journal of the Chemical Society, Chemical Communications., (16)578-580.
5. Pratt, C., 2006. "Applications of conducting polymers." Oxford University Press.
6. Scrosati, B.,1993. "Applications of electroactive polymers." Springer.
7. Rahman, M.A.,2008. "Electrochemical sensors based on organic conjugated polymers." Sensors., 8(1)118-141.
8. Orton, J.W., 2004. The story of semiconductors. Oxford University Press.
9. Atkins. P.W and J. D. Paula, 2009. Physical Chemistry. 9th ed . Oxford University Press.
10. Cheng,Y J., S.H. Yang and C.S. Hsu., 2009. "Synthesis of conjugated polymers for organic solar cell applications." Chemical reviews., 109(11), 5868-5923.
11. Daintith. J and E. Martin., 2005. Oxford Dictionary of Science. Oxford University Press.
12. Ramanathan. K. B., M. A Yun ., M. Chen., W. Mulchandan and A. Myung ., 2004. "Individually addressable conducting polymer nanowires array" Nano Letters., (4)1237-1239.
13. Rennert, P and D. Jiles., 1994. " Introduction to the Electronic Properties of Materials." Wiley Online Library.

14. Skotheim, T.A and J. Reynolds ., 2007. Handbook of Conducting Polymers, 2 Vols., CRC press.
15. MacDiarmid, A. and A.J. Epstein., 1994. " The concept of secondary doping as applied to polyaniline." Synthetic metals., 65(2),103-116.
16. Shimano, J.Y and A.G. MacDiarmid., 2001. "Polyaniline, a dynamic block copolymer: key to attaining its intrinsic conductivity." Synthetic Metals.,123(2), 251-262.
17. Green, A.G. and A.E. Woodhead., 1912. "Aniline-black and allied compounds. Part II." Journal of the Chemical Society., (101)1117-1123.
18. Masdarolomoor F., 2006. Novel nanostructured conducting polymer systems based on sulfonated polyaniline. Ph.D. Thesis, University of Wollongong.
19. De Albuquerque, J.M., L.H.C Faria., R.M Masters and J.G MacDiarmid., 2004. "Study of the interconversion of polyaniline oxidation states by optical absorption spectroscopy." Synthetic Metals., 146(1), 1-10.
20. Yue, J.E and MacDiarmid A.G., 1990. "Sulfonic acid ring-substituted polyaniline, a self-doped conducting polymer." Molecular Crystals and Liquid Crystals., 189(1), 255-261.
21. Bhadra, S.K., D. Singha, N.K Lee and J. Hee. 2009. "Progress in preparation, processing and applications of polyaniline." Progress in Polymer Science., 34(8), 783-810.
22. Kohlman, R., D.B. Tanner., C.G. Ihas., T. Ishiguro., Y.G. Min., A.G. MacDiarmid and A. Epstein.1997. Phys. Rev. Letters., (78) 3915-3918.
23. Wallace, G.G.,(ed), 2008. Conductive electroactive polymers: intelligent polymer systems.3rd. CRC press.
24. Molapo, K.N., P. Ajayi., R. Mbambisa., G. Mailu., S. Njomo., N.Masikini., M. Baker and E. Iwuoha. 2012. "Electronics of conjugated polymers (I): polyaniline." International Journal of Electrochemical Science., (**7)**11859-11875.
25. Yu, G. G., J. Hummelen., J. C. Wudl and F. Heeger., 1995. "Polymer photovoltaic cells: enhanced efficiencies via a network of internal donor-acceptor heterojunctions." Science-AAAS-Weekly Paper Edition., 270(5243).,1789-1790.
26. Janata, J. and M. Josowicz., 2003. " Conducting polymers in electronic chemical sensors." Nature materials., 2(1).,19-24.

27. Seyma, K.F., J. Shiokawa and S. Suzuki., 1983. " Proceedings of the International Meeting on Chemical Sensors." Fukuoka, Japan, September 19-22, 1983.
28. Hughes, R.C., A. J. Butler and M. A Martin ., 2004. "Sensors." Kirk-Othmer Encyclopedia of Chemical Technology.
29. Vasapollo,G., G. Sole., R. D. Mergola., L. Lazzoi., M. Rosaria., A. Scorrano and S. Mele ., 2011. "Molecularly imprinted polymers: present and future prospective." International journal of molecular sciences., 2(9), 5908-5945.
30. Cameron A., Lars I., Richard J., Nicole K., John O and M.J. Whitcombe. 2006. "Molecular imprinting science and technology: a survey of the literature for the years up to and including 2003. " J. Mol. Recognit., 6(19), 106–180.
31. Wulff, G. and A. Sarhan., 1972. "The use of polymers with enzyme-analogous structures for the resolution of racemates." Angew. Chem., 11, 341.
32. Umpleby II, R.J., Bode, M and K.D.Shimizu., 2000. "Measurement of the continuous distribution of binding sites in molecularly imprinted polymers." Analyst. , 125, 1261-1265.
33. Zhou, W., W.H. Lu., C.H. Guo., X. C. Chen., F. Yang., H.H. Wang and X. Ru .2010., "Mussel-inspired molecularly imprinted polymer coating superparamagnetic nanoparticlesforproteinrecognition." J.Mater.Chem., 20(5), 880-883.
34. Ye, L., R. Weiss, and K. Mosbach., 2000. "Synthesis and characterization of molecularly imprinted microspheres." Macromolecules., 33(22), 8239-8245.
35. Sellergren, B. and L. Andersson., 1990. "Molecular recognition in macroporous polymers prepared by a substrate analog imprinting strategy." The Journal of Organic Chemistry., 55(10), 3381-3383.
36. Mayes, A.G. and K. Mosbach., 1996. "Molecularly imprinted polymer beads: suspension polymerization using a liquid perfluorocarbon as the dispersing phase." Analytical Chemistry., 68(21),3769-3774.
37. Umpleby II, R.J., M. Bode, and K.D. Shimizu., 2000. "Measurement of the continuous distribution of binding sites in molecularly imprinted polymers." Analyst., 125(7), 1261-1265.

38. Reis, C.P.N., R. J. Ribeiro and A. J Veiga., 2006. "Nanoencapsulation I. Methods for preparation of drug-loaded polymeric nanoparticles." Nanomedicine: Nanotechnology, Biology and Medicine., 2(1), 8-21.

39. Thickett, S.C. and R.G. Gilbert, Emulsion polymerization. 2007. "State of the art in kinetics and mechanisms." Polymer., 48(24), 6965-6991.

40. Ruckenstein, E. and Y. Sun., 1995. "Polyaniline containing electrical conductive composite prepared by two inverted emulsion pathways." Synthetic metals., 74(2), 107-113.

41. Jang, J., J. Ha, and S. Kim., 2007. "Fabrication of polyaniline nanoparticles using microemulsion polymerization." Macromolecular Research., 15(2), 154-159.

42. Pourfarzib, M. S., M. Rastegar., A.A. Hossein., B. Mehramizi and A. D. Rassoul., 2015. "Molecularly imprinted nanoparticles prepared by miniemulsion polymerization as a sorbent for selective extraction and purification of efavirenz from human serum and urine." Journal of Chromatography B., 974(0),1-8.

43. Gao, D., Z. Zhongping., W. Minghong., X. Chenggen., G. Guijian and W. Dapeng., 2007. "A surface functional monomer-directing strategy for highly dense imprinting of TNT at surface of silica nanoparticles.'' Journal of the American Chemical Society., 129(25), 7859-7866.

44. Poma, A., 2012. Automatic solid-phase synthesis of molecularly imprinted nanoparticles (MIP NPs). Ph.D. Thesis, Cranfield University.

45. Vaihinger, D.L., K. Kräuter., I. Brunner., H. Tovar and E.M. Günter., 2002. "Molecularly imprinted polymer nanospheres as synthetic affinity receptors obtained by miniemulsion polymerisation." Macromolecular Chemistry and Physics., 203(13), 1965-1973.

46. Curcio, P., C. Zandanel, A. Wagner,C. Mioskowski and R. Baati. 2009. "Semi-covalent surface molecular imprinting of polymers by one-stage mini-emulsion polymerization: glucopyranoside as a model analyte." Macromol. Biosci., 9, 596-604.

47. Zeng, Z.H., Y. Rodriguez., A. Yoo and H. Shea. 2009. "Synthetic polymer nanoparticles with antibody-like affinity for a hydrophilic peptide." ACS nano., 4(1),199-204.

48. Dvorakova, G. H., R. Chiad., K. Klapper., M. Müllen and K. Biffis., 2013. "Molecularly imprinted nanospheres by nonaqueous emulsion polymerization." Macromolecular rapid communications., 31(23), 2035-2040.

49. Seyed M. M., and S. H. Hosseini., 2012. " Preparation of a Sensor of Imprinting Molecular Polymer Based on Polyaniline to recognise Agricultural Toxin Chlorpyrifos and Diazinon.'' Life Science Journal., 9(2), 1280-1285.

50. Tamayo, F., J. Casillas, and A. Martin-Esteban., 2005. "Evaluation of new selective molecularly imprinted polymers prepared by precipitation polymerisation for the extraction of phenylurea herbicides." Journal of chromatography A., 1069(2), 173-181.

51. Rao, T.P., K. Kala., R. Gladis and J. Mary., 2007. "Biomimetic sensors for toxic pesticides and inorganics based on optoelectronic/electrochemical transducers - An overview." Critical Reviews in Analytical Chemistry., 37(3),191-210.

52. D'Agostino, G., G. Alberti., R. Biesuz and M. Pesavento., 2006. "Potentiometric sensor for atrazine based on a molecular imprinted membrane." Biosensors and Bioelectronics., 22(1), 145-152.

53. Gong, J.G., F. Kuang., Y. Zeng., G. Shen and G. Yu., 2004. "Capacitive chemical sensor for fenvalerate assay based on electropolymerized molecularly imprinted polymer as the sensitive layer." Analytical and bioanalytical chemistry., 379(2), 302- 307.

54. Sanagi, M.M., 2013. "Molecularly imprinted polymer solid-phase extraction for the analysis of organophosphorus pesticides in fruit samples." Journal of Food Composition and Analysis., 32(2), 155-161.

55. Vien. D.L .,W.G. Fateley.,J.G. Graselli., 1991. The Handbook of Infrared and Raman Charcteriststic Frequencies of Organic Molecules.Academic Press., San Diego.

56. Harada. I ., Y. Furukawa and F. Udeda., 1989. Syth. Met, E303.

57. Chiang. J. C. 1986. Synth. Met., (13)193.

58. Koul.S ., S. Chandra.S and R. Chandra.1997. Indian J.Chem., (36A)901.

59. Huang. S .W. 1993. Polymer international., 34(9).

60. Silvestein. R.M., 2002. Spectroscopic Identification of Organic Compounds. John Wiley., Singapore.

61. Mooney, E.F.1971. Annual Reports on NMR Spectroscopy APL., Elsevier Science.

62. Laska . J and A. Pron. 1993. Mater.Sci.Forum., (177)177.

63. Wan . M. X. 1992. J. polym.sci part A., (30) 543.

64. Yan, F. and G. Xue. 1999. "Synthesis and characterization of electrically conducting polyaniline in water–oil microemulsion." Journal of Materials Chemistry., 9(12), 3035-3039.

65. Bańka, E. and W. Łużny., 1999. "Structural properties of polyaniline protonated with camphorsulfonic acid." Synthetic Metals., 101(1–3), 715-716.

# APPENDIX A

**Quantitative analysis of Aldrin and 1,1,1-trichloro-2,2-bis(*p*-chlorophenyl)ethane (DDT) in solutions by GC-TOFMS.**

## A.1 Calibration graph for Aldrin and DDT.

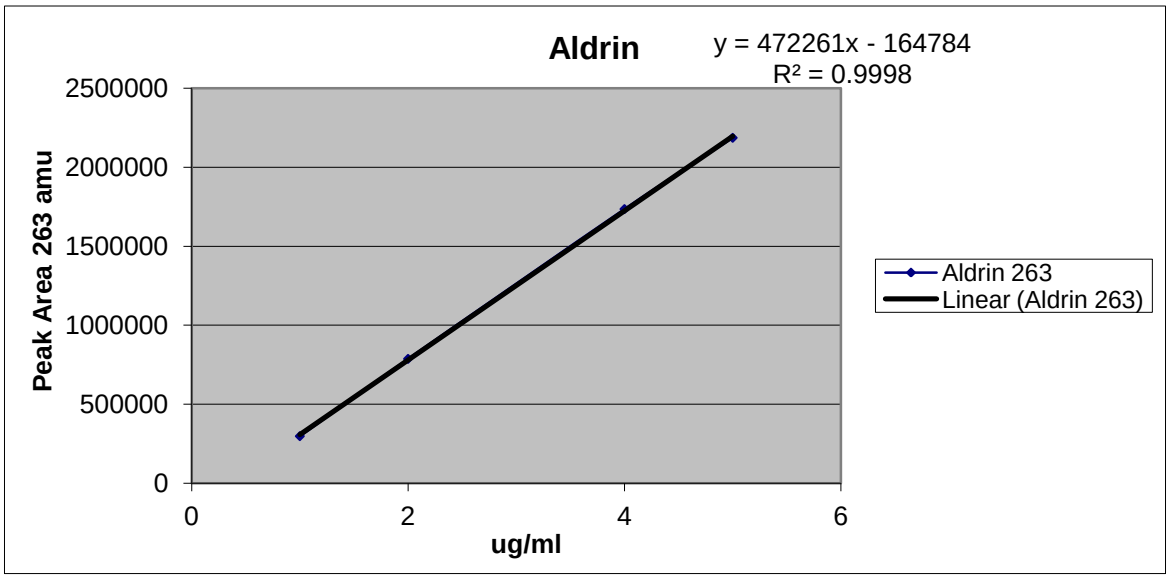


**Figure 1: Calibration graph for Aldrin.**

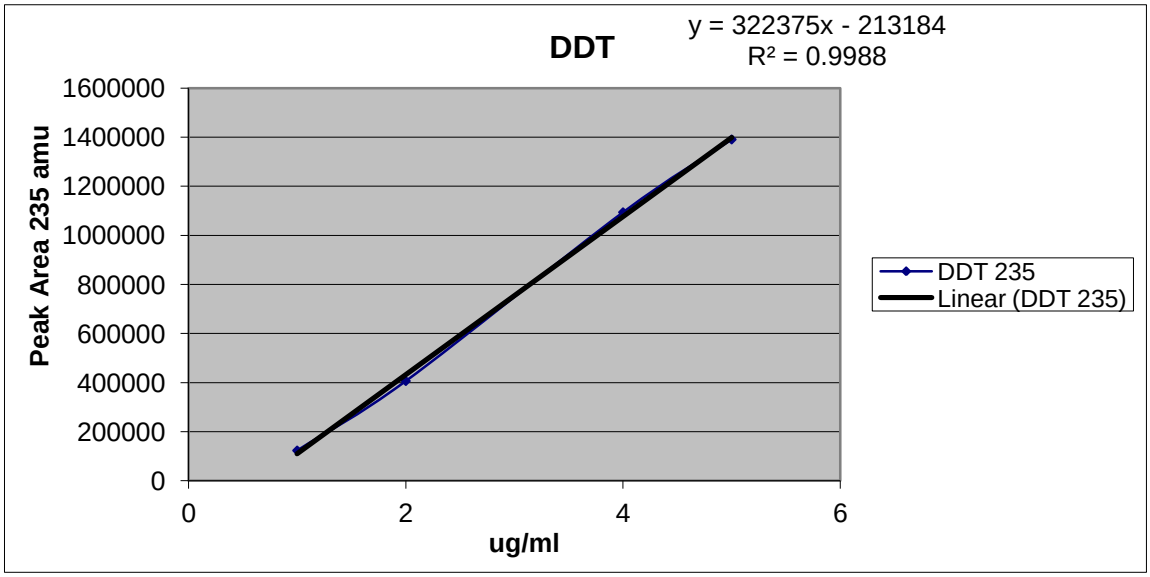


**Figure 2: Calibration graph for DDT.**

# A.2 Reconstructed ion chromatograms.

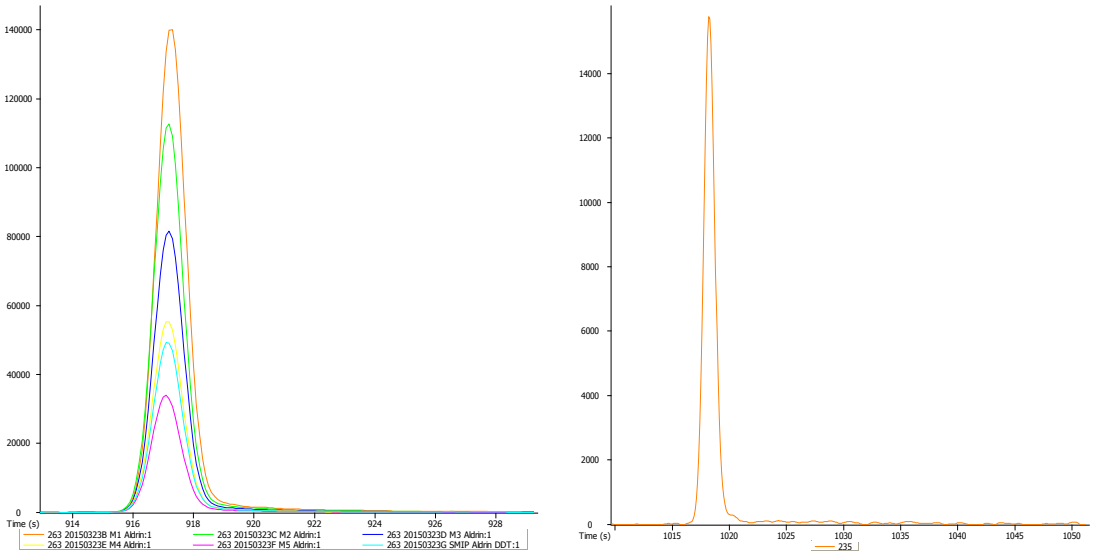


**(a)** **(b)**

**Figure 3: Reconstructed ion chromatogram (a) (263 Da) of Aldrin in M1 to M5 and SMIP, (b) (235 Da) of DDT in SMIP.**

# APPENDIX B

## FTIR Characterisation

### B.1 Aldrin FTIR spectra

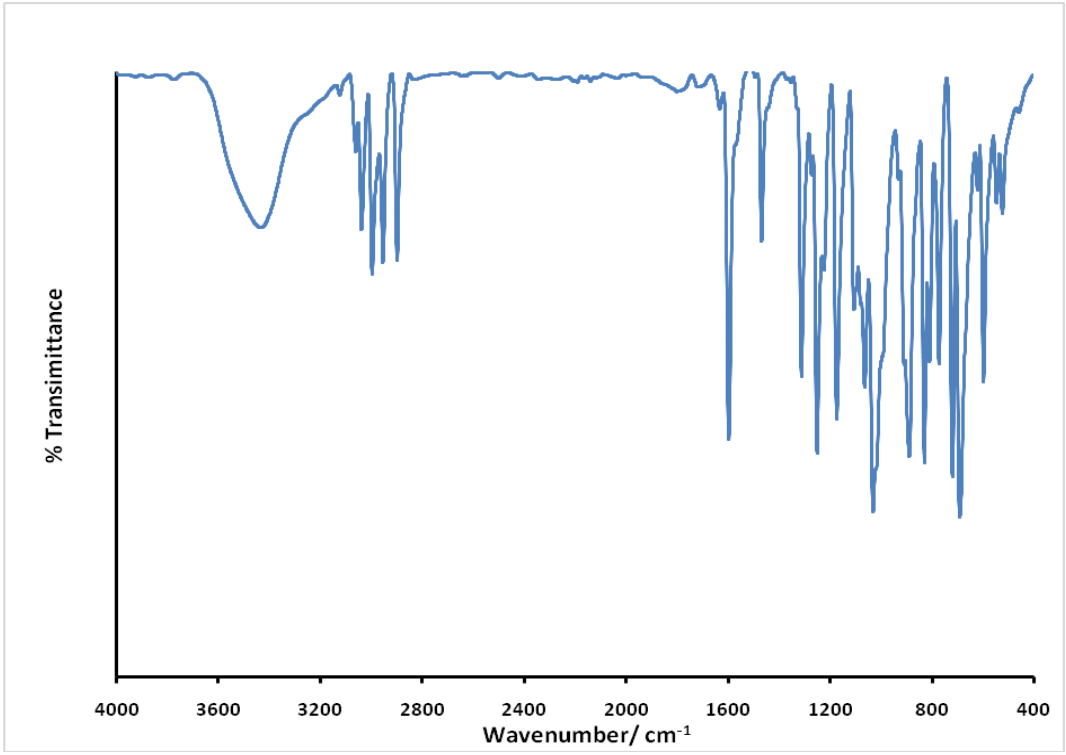


**Figure 4: FTIR spectra of aldrin.**

# PUBLICATIONS

1. Mbozi, A., M.O Munyati., M.N Siamwiza and M. Diale. 2016. “Molecularly Imprinted Polyaniline Nanoparticles for Selective Recognition of Aldrin: Synthesis and Characterisation.”Journal of Sensors and actuators: B.
2. Munyati, M.O., A. Mbozi., M.N Siamwiza and M. Diale. 2016. “Molecularly Imprinted Polyaniline Nanoparticles for Selective Recognition of Aldrin: Binding Capacity and selectivity”. Journal of Sensors and actuators: B.